

# REPORT DOCUMENTATION PAGE

Form Approved  
OMB No. 0704-0188

Public reporting burden for this collection of information is estimated to average 1 hour per response, including the time for reviewing instructions, searching data sources, gathering and maintaining the data needed, and completing and reviewing the collection of information. Send comments regarding this burden estimate or any other aspect of this collection of information, including suggestions for reducing this burden to Washington Headquarters Service, Directorate for Information Operations and Reports, 1215 Jefferson Davis Highway, Suite 1204, Arlington, VA 22202-4302, and to the Office of Management and Budget, Paperwork Reduction Project (0704-0188) Washington, DC 20503.

PLEASE DO NOT RETURN YOUR FORM TO THE ABOVE ADDRESS.

1. REPORT DATE (DD-MM-YYYY) 18-02-2002	2. REPORT DATE 18-02-2002	3. DATES COVERED (From - To) 15-02-1999 - 30-09-2001
---	------------------------------	---

4. TITLE AND SUBTITLE  Theory and simulation of moletronics devices and systems	5a. CONTRACT NUMBER
	5b. GRANT NUMBER N00014-99-1-0351
	5c. PROGRAM ELEMENT NUMBER

6. AUTHOR(S)  Sokrates T. Pantelides	5d. PROJECT NUMBER 99PRO4333-00
	5e. TASK NUMBER
	5f. WORK UNIT NUMBER

7. PERFORMING ORGANIZATION NAME(S) AND ADDRESS(ES)  Vanderbilt University Nashville, TN 37235	8. PERFORMING ORGANIZATION REPORT NUMBER
--	--

9. SPONSORING/MONITORING AGENCY NAME(S) AND ADDRESS(ES)  Office of Naval Research/John Pazik ONR331, Ballston Centre Tower One 800 North Quincy Street Arlington, VA 22217	10. SPONSOR/MONITOR'S ACRONYM(S)  ONR
	11. SPONSORING/MONITORING AGENCY REPORT NUMBER

12. DISTRIBUTION AVAILABILITY STATEMENT  
  
Approved for Public Release; Distribution is Unlimited

13. SUPPLEMENTARY NOTES

14. ABSTRACT  
  
Suitable methods were developed and used to simulate the transport properties of moletronics devices in the context of experimental data obtained by other teams in the MOLETRONICS Program. Several molecular devices were simulated successfully, explaining the data and providing information on the mechanisms that control the observed properties. Several predictions were made about devices that are yet to be fabricated.

15. SUBJECT TERMS

16. SECURITY CLASSIFICATION OF:			17. LIMITATION OF ABSTRACT	18. NUMBER OF PAGES	19a. NAME OF RESPONSIBLE PERSON
a. REPORT	b. ABSTRACT	c. THIS PAGE			Sokrates T. Pantelides
					19b. TELEPHONE NUMBER (include area code) (615) 343-4321

20020319 203

**Final Report**  
***“Theory & Simulation of Moletronics Devices & Systems”***  
**DARPA Grant. No. N00014-99-1-0351**

**Sokrates T. Pantelides, Principal Investigator**

**TECHNICAL SUMMARY**

The project’s primary objective was to develop suitable theoretical methods to simulate the transport properties of individual molecules and provide information about the mechanisms that control these properties in the context of efforts to develop “moletronic” devices and systems by other teams in the Moletronics Program. The task was accomplished: state-of-the-art methods were developed that allow the calculation of the current voltage characteristics of individual molecules and include current-induced atomic relaxations and motions; the methods were employed for a series of molecules that were fabricated and measured by the team headed by Mark Read and James Tour. The experimental observations were accounted for and the underlying mechanisms that control the properties of the molecule were identified. In addition, three-terminal devices, not yet fabricated but necessary for functional systems, were simulated and predictions were made. The results were published in five articles in premier journals and several Conference Proceedings. A summary of the results is given in this report and the original articles are attached as Appendices.

**INTRODUCTION**

Silicon-based microelectronics is reaching the level of miniaturization where quantum phenomena such as tunneling cannot be avoided and the control of doping in ultrasmall regions becomes problematical. Though it is likely that silicon-based technology will simply move to a different paradigm and continue taking advantage of the existing vast infrastructure and manufacturing capabilities, novel and alternative approaches may give new insights and ultimately may usher a new era in nanoelectronics. Molecules as individual active devices are obvious candidates for the ultimate ultrasmall components in nanoelectronics. Though the idea has been around for more than two decades,<sup>1</sup> only recently measurements of current-voltage characteristics of individual molecules have been feasible. There have been significant breakthroughs in experimental measurements that offer considerable promise.<sup>2-7</sup>

Methods for the calculation of current in small structures placed between two metal electrodes have been developed over the years, but actual implementations have been scarce. For molecules, semiempirical methods have been used to

study the dependence of current on various aspects of the problem,<sup>8</sup> but quantitative predictions for direct comparison with data are not possible because values of parameters under current conditions cannot be determined independently.

In the 1980's, Lang developed a practical method to calculate transport in the context of imaging atoms with scanning tunneling microscopy.<sup>9</sup> The method has all the ingredients needed to compute current-voltage (I-V) characteristics of single molecules. We adopted this method and, in addition, we developed a suitable Hellmann-Feynman theorem for the calculation of current-induced forces on atoms that allows us to study the effect of current on relaxations and ultimately the breakdown of molecules.<sup>10</sup> With these tools, we have carried out extensive studies of transport in molecules whose core is a single benzene ring. Such molecules have been synthesized and measured by Reed and coworkers.<sup>2,3</sup> Here, we summarize the most important results of the recent work. The method of calculation and more details of the results can be found in the original papers.<sup>11-14</sup>

### TRANSPORT IN A SINGLE BENZENE RING

Most of our theoretical work has been carried out on single benzene rings because the small number of atoms makes the calculations practical. Experimental data are available for two-terminal configurations.

Fig. 1 shows schematics of a single benzene ring bridging the gap between macroscopic gold electrodes. A sulfur atom at each end joins the benzene ring to the electrodes. The experimental I-V characteristic is shown in the top panel. The middle panel shows the theoretical results.<sup>11</sup> We will discuss the third panel shortly.

It is clear from the figure that the theory reproduces the shape of the I-V curve quite well, but the absolute magnitude of the current is off by more than two orders of magnitude. We address each of these issues separately.

In Fig. 2 we show the density of states of the molecule for three different voltages: 0.01 V, 2.4 V and 4.4 V and mark out the energy window between the left and right quasi Fermi levels. States within this window contribute to transport. We see that there is virtually no density of states in the small window at small voltages, in agreement with the slow initial rise of the I-V curve. At 2.4 V, the  $\pi^*$  states of the molecule enter the transport window and give rise to the first peak in the spectrum. At 4.4 V, the  $\pi$  states of the molecule enter the window while the  $\pi^*$  continue to participate, giving rise to the second peak in the spectrum. The peak at 2.4 V is somewhat more pronounced in the theoretical curve. The observed smoothing is likely to be caused by interactions between the electrons and vibrational modes.

In order to explore the mechanism that controls the absolute magnitude of the current we performed calculations by inserting an extra gold atom between the sulfur atom and the macroscopic electrode at each end of the molecule as

shown in the lower part of Fig. 1. There was a dramatic decrease in the current, bringing its value much closer to the experimental value (lower panel in Fig. 1). The decrease is attributed to the fact that gold atoms have only one  $s$  electron available for transport and  $s$  electrons do not couple with the  $\pi$  electrons of the molecule. The gold atoms act as a quantum mechanical constriction. To test the idea we performed calculations by replacing the gold atoms with aluminum atoms. The latter have  $p$  electrons that should couple well with the  $\pi$  electrons of the molecule. Indeed, the current jumped to its initial value. An additional test was carried out with three gold atoms instead of a single gold atom. The current was again at its full value because the three  $s$  orbitals on the three gold atoms can form the appropriate linear combinations to produce sufficient coupling.

It is clear from the above that molecules determine the shape of the I-V characteristic, but the nature of individual atoms at the molecule-electrode contact determines the absolute magnitude of the current. The results illustrate the power of theory to contribute to device design, especially “contact engineering”.

### A THREE-TERMINAL DEVICE

Transistor-like behavior in molecular three-terminal devices (molecular transistors) has been recently demonstrated in a single  $C_{60}$  bucky ball connected to gold electrodes,<sup>4</sup> in organic self-assembled monolayers,<sup>5</sup> and in single and multi-walled carbon nanotubes.<sup>6,7</sup> The source-drain current in these systems (three-terminal devices) is controlled by a gate voltage.

As an example of a three-terminal device we considered the same benzene ring as above but put a third “terminal” in the form of a capacitive gate: an external electric field across the molecule produces polarization that affects the current through the molecule. Figure 3 shows that at a very small (0.01 V) source-drain voltage, the current is a strong function of the gate voltage. In particular, we demonstrate substantial gain at the resonant peak.

Recently, we explored the effect of symmetry on the current-gate-field (I-E) characteristics of model molecular transistors. In particular, we investigated the role of intrinsic dipole moments on the current modulation in these structures. Figure 3 shows the two core molecules that have been constructed from the benzene-1,4-dithiolate molecule by substituting one of two hydrogen molecules by hydroxile groups (OH). The transport properties in these two molecules were found to be very different. The amplification of the current at the resonant tunneling regime is a few times larger in the asymmetric molecule which is a subject to a linear Stark effect in the gate electric field. At the same time, resonant tunneling occurs at much lower voltage than in the symmetric molecule.

The shape of the I-E characteristics depends on the value of the source-drain voltage in a nonlinear way, thus manifesting a strong dependence between the source-drain current and the gate electric field. These results illustrate that substituents and symmetry considerations can provide considerable control of the behavior of molecular transistors. Further discussion of the results can be found in the original papers.<sup>12,14</sup>

### TEMPERATURE EFFECTS IN MOLECULAR DEVICES

Chen et al.<sup>3</sup> recently reported I-V characteristics of molecules consisting of chains of three benzene rings with ligands attached at various places. The most interesting result is large negative differential resistance evinced by a relatively sharp spike in the I-V characteristic. The spike is found to broaden and shift on the voltage axis with increasing temperature. The shift, by about 1 V, is very unusual. In semiconductor nanostructures resonant peaks have been found to broaden (by standard electron-phonon interactions) but they never shift appreciably.

Calculations for three-benzene-ring molecules are not practical, but we pursued the question by calculations for a single benzene ring with an NO<sub>2</sub> ligand replacing one of the hydrogen atoms.<sup>13</sup> We found that the energy levels of the ligand move substantially with increasing voltage and push the  $\pi$  levels into the active window. Thus the main peak in the current arises primarily from  $\pi$  electrons instead of  $\pi^*$  electrons. We then explored the effect of rotating the ligand. We found that a rotation by 90° shifts the peak to lower voltage by almost 1 V, in agreement with observations (Fig. 4). The interpretation is that higher temperatures excite the rotational modes of the ligand. Calculations of the total energy of the molecule as a function of ligand rotation show that the effective rotational quantum of energy is only 3 meV. Thus, even at the relatively low temperatures of the experiment, a large number of quanta are excited, making the ligand effectively a classical rotor that spends most of its time at the extrema of the amplitude. Ligand rotation is of course a unique phenomenon of the molecular world, explaining why large voltage shifts are not observed in semiconductor nanostructures.

### CONCLUSIONS

The calculations summarized above show that theory has now advanced to the point where quantitative predictions can be made about transport in single molecules. Such calculations are expected to play a major role in the evolution of molecular electronics, the way that simple drift-diffusion calculations of current in semiconductor structures have played in the evolution of silicon-based microelectronics.

Acknowledgement: This work was supported in part by a grant from DARPA/ONR, by the National Science Foundation and by the William A. and Nancy F. McMinn Endowment at Vanderbilt University.

## REFERENCES

- [1] A. Aviram and M. A. Ratner, “*Molecular Rectifiers*”, Chem. Phys. Lett. 29, 277 (1974). See also *Molecular Electronics*, edited by A. Aviram and M. A. Ratner (New York Academy of Sciences, New York, 1998).
- [2] M. A. Reed, C. Zhou, C. J. Muller, T. P. Burgin, and J. M. Tour, Science 278, 252 (1997).
- [3] J. Chen, M. A. Reed, A. M. Rawlett, and J. M. Tour, Science 286, 1550 (1999).
- [4] H. Park, J. Park, A. K. L. Lim, E. H. Anderson, A. P. Alvisatos, and E. P. McEuen, Nature 407, 57 (2000).
- [5] J. H. Schon, H. Meng, and Z. Bao, Nature 413, 713 (2001).
- [6] J. W. G. Wildoer, L. C. Venema, A. G. Rinzler, R. E. Smalley, and C. Dekker, Nature (London) 391, 59 (1998).
- [7] R. Martel, T. Schmidt, H. R. Shea, T. Herzog, and Ph. Avouris, Appl. Phys. Lett. 73, 2447 (1998).
- [8] S. Datta, W. Tian, S. Hong, R. Reifenberger, J. I. Henderson, and C. P. Kubiak, Phys. Rev. Lett. 79, 2530 (1997); S. N. Yaliraki, A. E. Roitberg, C. Gonzales, V. Mujica, and M. A. Ratner, J. Chem. Phys. 111, 6997 (1999); J. K. Gimzewski and C. Joachim, Science 283, 1683 (1999).
- [9] See N. D. Lang, Phys. Rev. B 52, 5335 (1995); *ibid.* 49, 2067 (1994).
- [10] M. Di Ventra and S. T. Pantelides, Phys. Rev. B 61, 16207 (2000).
- [11] M. Di Ventra, S. T. Pantelides, and N. D. Lang, Phys. Rev. Lett. 84, 979 (2000).
- [12] M. Di Ventra, S. T. Pantelides, and N. D. Lang, Appl. Phys. Lett. 76, 3448 (2000).
- [13] M. Di Ventra, S.-G. Kim, S. T. Pantelides and N. D. Lang, Phys. Rev. Lett. 86, 288 (2001)
- [14] S. N. Rashkeev, M. Di Ventra, and S. T. Pantelides, Phys. Rev. Lett. (submitted).

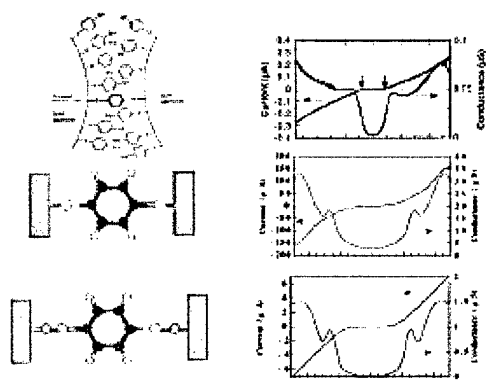


Fig. 1 Schematics of benzene ring configurations between electrodes and I-V characteristics. Top row: Experiment (Ref. 5). Middle row: Theory with S atoms only between benzene ring and macroscopic electrodes (Ref. 7). Lower row: Theory with Au atoms inserted between the S atoms and the macroscopic electrodes (Ref. 7).

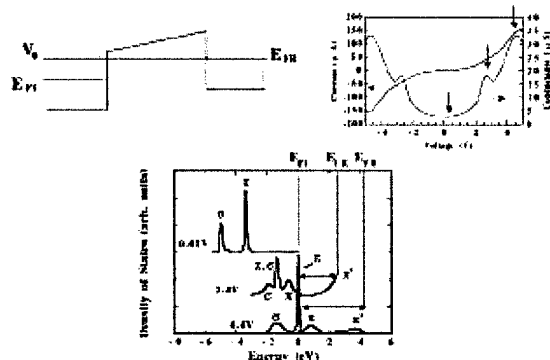


Fig. 2 Schematic of the setup showing the left and right quasi-Fermi levels; the I-V characteristic as in Fig. 1, and the densities of states discussed in the text.

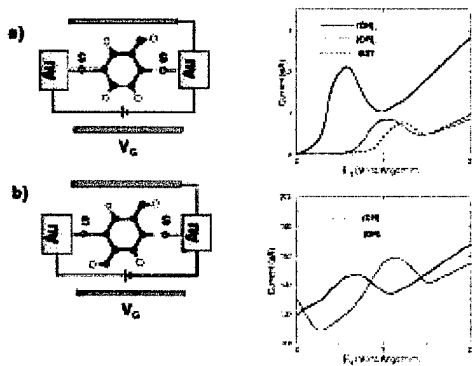


Fig. 3 Schematic of three-terminal devices using two different molecules as discussed in the text and the theoretical I-V characteristics as a function of the gate voltage for a small source-drain voltage.

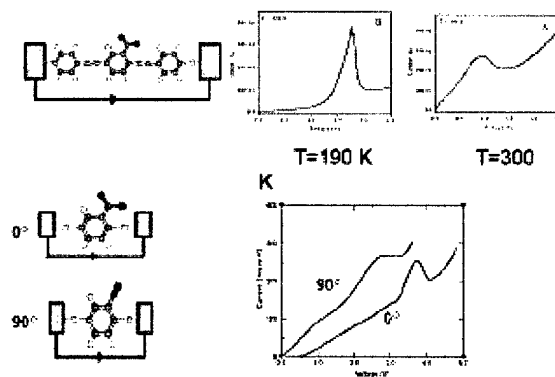


Fig. 4 Experimental data by Chen et al. (Ref. 6) at two temperatures and theoretical I-V curves for two different orientations of the ligand. See text for more details.

## PAPERS REPORTING ORIGINAL WORK

M. Di Ventra, S. T. Pantelides, and N. D. Lang, "First-Principles Calculation of Transport Properties of a Molecular Device", *Phys. Rev. Lett.* **84**, 979 (2000).

M. Di Ventra, S. T. Pantelides and N. D. Lang, "The Benzene Molecule as a Molecular Resonant-Tunneling Transistor", *Appl. Phys. Lett.* **76**, 3448 (2000).

M. Di Ventra and S. T. Pantelides, "Hellmann-Feynman Theorem and the Definition of Forces in Quantum Time-Dependent and Transport Problems", *Phys. Rev. B* **61**, 16207 (2000).

M. Di Ventra, S.-G. Kim, S. T. Pantelides and N. D. Lang, "Temperature Effects on the Transport Properties of Molecules", *Phys. Rev. Lett.* **86**, 288 (2001).

M. Di Ventra, S. T. Pantelides, and N. D. Lang, "Current-Induced Forces in Molecular Wires", *Phys. Rev. Lett.* **88**, 6801(2002).

## OTHER PUBLICATIONS

M. Di Ventra, S. T. Pantelides and N. D. Lang, "Ab-Initio Simulation of Transport Properties of Molecular Structures", p. 639 in *Cluster and Nanostructure Interfaces*, ed. by P. Jena, S. N. Khanna, and B. K. Rao, World Scientific, Singapore (1999).

S. T. Pantelides, M. Di Ventra, S. G. Kim, and N. D. Lang, "The Behavior of Molecules as Electronic Devices", *Envision* **16**, 18 (2000).

M. Di Ventra, N. D. Lang, and S. T. Pantelides, "Transport Calculations in Molecular Devices from First Principles" in *Molecular Electronics*, edited by S. T. Pantelides, M. A. Reed, J. S. Murday, and A. Aviram, MRS Symposium 582, H3.3.1 (2000).

S. T. Pantelides, M. Di Ventra and N. D. Lang, "Molecular Electronics by the Numbers", *Physica B* **296**, 72 (2001).

S. T. Pantelides, M. Di Ventra, N. D. Lang, and S. N. Rashkeev, "Molecular Electronics By The Numbers", *IEEE Trans. Elec. Dev.*, in press.

S. T. Pantelides, M. Di Ventra, N. D. Lang, "First-Principles Simulations of Molecular Electronics", *Molecular Electronics II*, Volume 960 of the *Annals of the New York Academy of Sciences*, edited by A. Aviram, M. Ratner, and V. Mujica, in press.

## INVITED TALKS AT CONFERENCES AND WORKSHOPS

"Ab-Initio Simulations of Electronic Transport in Molecular Nanostructures", M. Di Ventra, N. D. Lang, and S. T. Pantelides, *International Symposium on Cluster and Nanostructure Interfaces*, Richmond, VA. October 1999.

"Ab-Initio Simulations of Molecular Electronic Devices", M. Di Ventra, N. D. Lang, and S. T. Pantelides, *Materials Research Society Meeting*, Boston, MA. November 1999.

"Ab-initio Simulation of Transport in Molecular Devices" M. Di Ventra, N. D. Lang, and S. T. Pantelides, *APS March Meeting*, Minneapolis, MN. March 2000.

"Electronic Transport in Molecules", *Symposium on the 60th Birthday of Prof. E. Economou*, Crete, June 2000.

"Ab Initio Simulations of Molecular Electronics", M. Di Ventra, N. D. Lang, and S. T. Pantelides, *NANOTECH 2000 Conference*, Houston, TX. Sept. 2000.

“Transport Calculations in Molecular Devices from First Principles”, M. Di Ventra, N. D. Lang, and S. T. Pantelides, Fall MRS Meeting, Boston, MA. Nov. 2000.

“Molecular Electronics by the Numbers“, Conference on Microelectronics, Microsystems, and Nanotechnology, Athens, Greece. Nov. 2000.

“Molecular Electronics by the Numbers“, Molecular Electronics 2000 Conference, Kona, HI. Dec. 2000.

“Molecular Electronics by the Numbers“, Computational Science Workshop, Tsukuba, Japan. March 2001.

“Modeling and Simulation of Molecular Electronic Devices“, ARDA Workshop on Molecular Electronics, College Park, MD. April, 2001.

“First Principles Simulations of Molecular Electronics”, M. Di Ventra, N. D. Lang, and S. T. Pantelides, Lakeview Conference, Morgantown, WV. May 2001.

“Molecular Electronics by the Numbers”, Nanoscience and Nanotechnology Conference, Atlanta, GA. Sept. 2001.

“Molecular Electronics by the Numbers“, Accelrys Seminar on Computational Nanotechnology, Washington, DC. Oct. 2001.

“Molecular Electronics by the Numbers “IUVSTA, American Vacuum Society Meeting, San Francisco, CA. Oct. 2001.

Forthcoming invited talks:

“First-principles theory of transport in molecules and multilayer nanostructures”, Meeting of the American Physical Society, Indianapolis, IN. March 2002.

“Molecular Electronics by the Numbers“, Conference on Carbon-based Molecular Electronics, Great Malvern, UK, April 2002.

“Molecular Electronics by the Numbers”, Joint Conference of ICCN 2002 and MSM 2002, San Juan, Puerto Rico, April 2002.

## First-Principles Calculation of Transport Properties of a Molecular Device

M. Di Ventra,<sup>1</sup> S. T. Pantelides,<sup>1,2</sup> and N. D. Lang<sup>3</sup>

<sup>1</sup>*Department of Physics and Astronomy, Vanderbilt University, Nashville, Tennessee 37235*

<sup>2</sup>*Solid State Division, Oak Ridge National Laboratory, Oak Ridge, Tennessee 37831*

<sup>3</sup>*IBM Research Division, Thomas J. Watson Research Center, Yorktown Heights, New York 10598*

(Received 20 April 1999)

We report first-principles calculations of the current-voltage ( $I$ - $V$ ) characteristics of a molecular device and compare with experiment. We find that the shape of the  $I$ - $V$  curve is largely determined by the electronic structure of the molecule, while the presence of single atoms at the molecule-electrode interface play a key role in determining the absolute value of the current. The results show that such simulations would be useful for the design of future microelectronic devices for which the Boltzmann-equation approach is no longer applicable.

PACS numbers: 73.40.Jn, 73.40.Cg, 73.40.Gk, 85.65.+h

Conventional Si-based microelectronics is likely to reach its limit of miniaturization in the next 10–15 years when feature lengths shrink below 100 nm. The main problem is the onset of quantum phenomena, e.g., tunneling, that would make scaled-down conventional devices inoperable. Successor technologies currently under development, such as tunneling field-effect transistors and single-electron transistors, are in fact based on quantum phenomena. For the ultimate miniaturization below nm, devices made from single molecules are currently attracting attention. Prototypes have already been fabricated. Reed *et al.* [1] reported  $I$ - $V$  characteristics of single benzene-1,4-dithiolate molecules. Alivisatos and co-workers [2] reported similar  $I$ - $V$  characteristics of semiconductor and metal nanoclusters between gold electrodes. Dekker and co-workers [3] reported transistorlike behavior in carbon nanotubes. Similar devices have been demonstrated by Avouris and co-workers using single-walled and multiwalled carbon nanotubes [4].

Theoretical modeling played a key role in the invention of the transistor and in the subsequent development of integrated circuits. Device modeling continues to provide indispensable input to circuit modeling for designing logic and memory chips and microprocessors. It is based on a “semiclassical approximation” that treats electrons and holes as classical particles, except that their kinetic energies are determined by the semiconductor energy bands, most commonly in the effective-mass approximation. In this scheme, transport is governed by Boltzmann’s equation. Most industrial modeling is done in the drift-diffusion approximation, to a lesser extent in the higher-order hydrodynamic approximation, and, at times, by solving Boltzmann’s equation directly by Monte Carlo techniques [5]. For nanodevices, however, when quantum phenomena are dominant, the semiclassical Boltzmann’s equation does not apply. Quantum mechanical simulations are needed. So far, only semiempirical approaches have been employed to investigate transport in molecular systems, providing useful insights into the fundamental mechanisms [6–9].

In this Letter we report first-principles calculations of the  $I$ - $V$  characteristics of a molecule. In this method, the electrostatic potentials through the molecule and at the contacts are calculated self-consistently without empirical adjustments. We report calculations for the benzene-1,4-dithiolate molecule for which experimental data are available [1]. We find that, when the molecule is placed between two electrodes made of an ideal metal (homogeneous electron gas or jellium model [10]), the shape of the  $I$ - $V$  characteristic is determined by the electronic structure of the molecule in contact with the electrodes and in the presence of the external electric field. The shape is essentially the same as that of the experimental curve. The absolute magnitude of the current, however, is more than 2 orders of magnitude larger than the experimental values. We investigated the origins of this discrepancy and found that insertion of a single gold atom at each metal-molecule contact, as suggested by the experimental setup, leaves the shape of the  $I$ - $V$  characteristic globally unchanged, but reduces the absolute value of the current by more than an order of magnitude, reflecting reduced coupling between the  $s$  states of the gold and the  $p$  orbitals of the molecule, in the directions parallel to the electrode surfaces. Replacement of the single gold atoms by aluminum atoms, which have  $p_z$  orbitals in the relevant energy region, raises the value of the current by about 1 order of magnitude. Other factors that can affect the absolute value of the current are discussed later in this paper. These results show that such calculations can provide valuable quantitative information to help design molecular devices.

We begin with the study of the  $I$ - $V$  characteristic of a single benzene-1,4-dithiol molecule between two ideal metallic contacts. It is well known that when the benzene-1,4-dithiol molecule is adsorbed on gold surfaces the  $H$  of the thiol terminations desorbs and the sulfur atoms at each end bond strongly to the Au(111) surfaces [11]. The remaining molecule (benzene-1,4-dithiolate) is then simply the one represented in Fig. 1, where we show the contour plot of the electronic density in the benzene ring plane. We

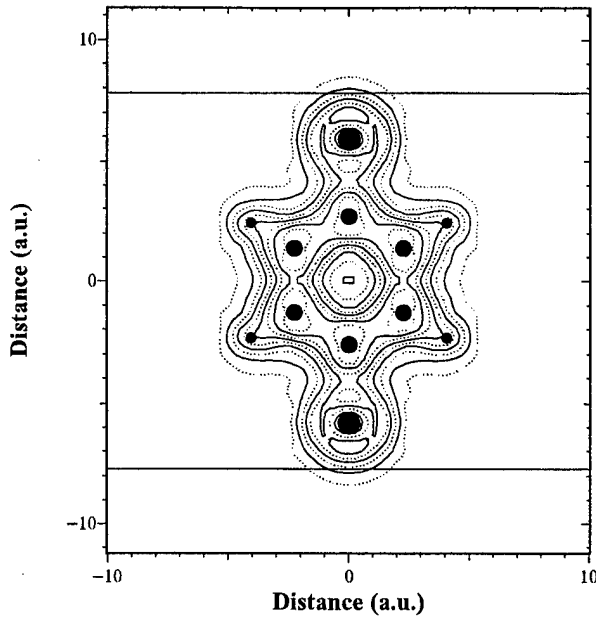


FIG. 1. Contour plot of the electron density of the molecule described in the text. The dots represent the positions of the atoms. The lines represent the position of the model metal surfaces.

assume that the molecule stands perpendicular to the metal surfaces. The molecule has  $\pi$  bonding and  $\pi^*$  antibonding orbitals formed by the carbon and sulfur  $p$  orbitals perpendicular to the ring plane and  $\sigma$  bonds due to the in-plane orbitals of the atoms.

We computed the  $I$ - $V$  characteristic using the method developed in Ref. [12]. The electron density of the jellium electrodes is taken equal to the value for metallic gold ( $r_s \approx 3$ ). The electron wave functions are computed by solving the Lippman-Schwinger equation iteratively to self-consistency in steady state. Exchange and correlation are included in the density-functional formalism within the local-density approximation [13]. All atomic positions are kept fixed at their equilibrium values in the free molecule. The current is computed from the wave functions of the electrode-molecule system. The differential conductance is then calculated as the derivative of the current with respect to the external bias. Small variations in the atomic positions (of the order of 0.1 Å) change the current by less than 1%.

The calculated  $I$ - $V$  characteristic is shown in the bottom panel of Fig. 2. The experimental curve is also shown for comparison in Fig. 2. It is clear that the shapes of the two curves are similar, but the absolute magnitude of the current and conductance is quite different. We will first discuss the origins of the shape and then address the question of absolute values.

We focus on three distinct regions in the calculated conductance curve: the initial rise (from zero bias to about 1 V), the first peak at 2.4 V, and the second peak at 4.4 V.

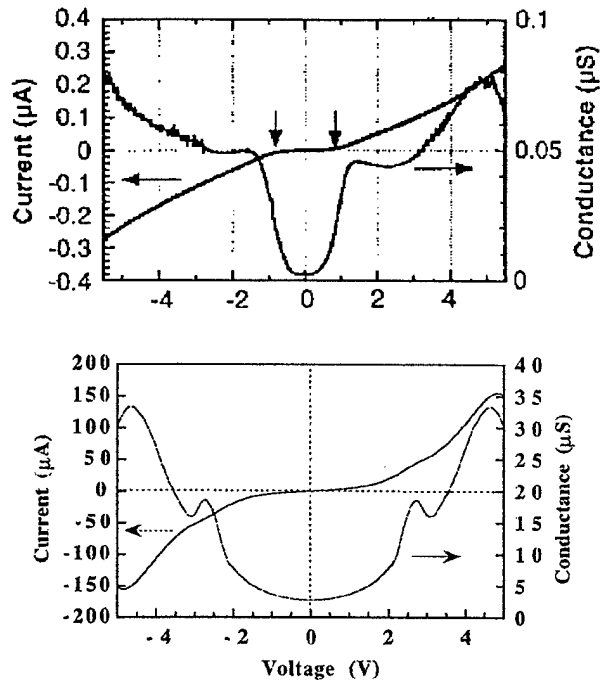


FIG. 2. Top: Experimental  $I$ - $V$  characteristic of a benzene-1,4-dithiolate molecule measured by Reed *et al.* [1]. Bottom: Conductance of the molecule of Fig. 1 as a function of the external bias applied to the metallic contacts.

In Fig. 3 we show the calculated density of states of the molecule for three different voltages, namely, 0.01, 2.4, and 4.4 V (the density of states shown is the difference between that of the molecule-electrode system and that of the electrodes without the molecule). The zero of energy is the left Fermi level so that the right Fermi level is equal

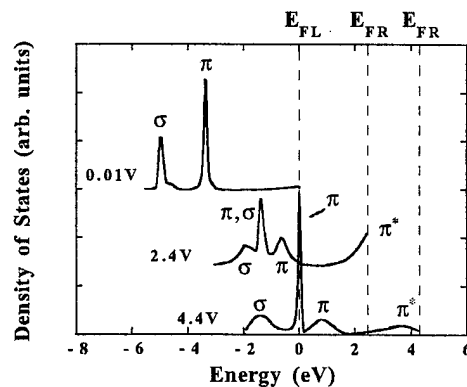


FIG. 3. Difference between the density of states of the two semi-infinite electrodes with and without the benzene-1,4-dithiolate molecule in between, for three different voltages. The left Fermi level ( $E_{FL}$ ) has been chosen as the zero of energy. The labels  $E_{FR}$  correspond to the energy position of the right Fermi levels. The three curves correspond to the bias voltages indicated.

to the external bias (in Fig. 3 the labels  $E_{FR}$  correspond to the 2.4 and 4.4 V values of the bias).

The initial slow rise of the conductance, which is also present in the experimental data, represents basically Ohmic behavior. Figure 3 (top curve) shows that the molecule has a small but relatively smooth density of states through which current can flow. The  $\sigma$  and  $\pi$  bonding states lie several eV below the Fermi energy so that a considerable bias is needed to produce nonlinear behavior.

After the initial increase of the current with increasing bias, a first conductance peak and subsequent valley are observed. This is also observed experimentally, though at somewhat lower voltages and with a smaller peak-to-valley ratio. The peak and the valley are due to *resonant tunneling* through  $\pi^*$  antibonding states, which are the first to appear in the window of energy between the right and left Fermi levels (see Fig. 3, middle curve). Inclusion of the vibrational coupling would smear out the peak and generate a lower peak-to-valley ratio in the  $I$ - $V$  characteristic, bringing closer the agreement between theory and experiment. Note also that the bonding  $\sigma$  and  $\pi$  states are altered significantly by the bias simply because the different atoms of the benzene ring are at different potentials.

Increasing the bias further, a second  $I$ - $V$  peak is found due to resonant tunneling with  $\pi$  bonding states. From Fig. 3 it is evident that the  $\pi^*$  antibonding states are still present in the energy region between the right and left Fermi levels but with a lower peak ratio with respect to the  $\pi$  bonding states. The discrepancy between the theoretical and experimental peak positions is consistent with known limitations of the local-density approximation [14].

The different scattering processes that occur for different biases can be studied in more detail by looking at the local density of states along the direction of current flow. The local density of states integrated between the left and right Fermi levels for small bias is plotted in Fig. 4(A). As in the case of the total density of states, we plot here the difference between the local density of states of the molecule-electrode system and that of the electrodes without the molecule. It is evident that the sulfur-to-metal contact has a very low density of states, in effect constituting a barrier through which electrons must tunnel. After tunneling through this barrier, the electrons encounter a region of relatively smooth, higher density of states corresponding to the states of the molecule. For biases in the neighborhood of 2.5 V [Fig. 4(B)], the electrons find a much larger density of states originating from the  $\pi^*$  antibonding states of the molecule (resonant tunneling condition). The antibonding region is between the middle carbons of the molecule. Finally, with a further increase of the bias, to the range of 5 V, resonant tunneling occurs through bonding states of the molecule [see Fig. 4(C)].

We now turn to the absolute value of the current which differs by more than 2 orders of magnitude from the experimental value. We attribute part of this discrepancy to the

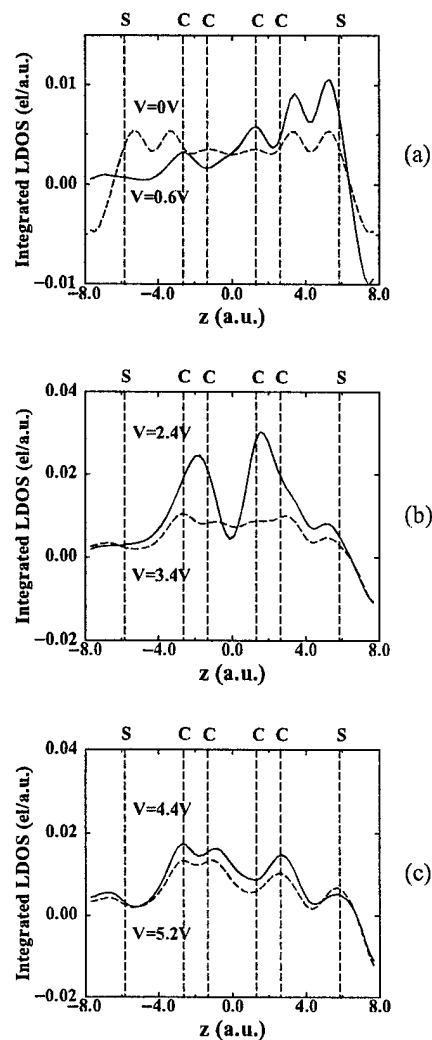


FIG. 4. Local density of states difference between that of the molecule-electrode system and that of the electrodes without the molecule, integrated between left and right Fermi levels. Voltage region (A) corresponds to the linear response regime. Region (B) corresponds to the first resonant tunneling. Region (C) corresponds to the second resonant tunneling bias conditions.

contact geometry and chemistry. The experiment by Reed *et al.* [1] suggests that the contacts are atomically terminated, which means that the sulfur atoms are attached to *single* Au atoms. We investigated the effect of such a possibility on the  $I$ - $V$  characteristic by introducing a single gold atom between the sulfur and the model metal surface at each contact. The shape of the  $I$ - $V$  characteristic (Fig. 5) remains essentially the same, but the absolute value of the conductance *decreases* by almost 2 orders of magnitude. This reduction is partly due to the constriction resistance generated by the *geometry* of the contact and partly due to the *chemistry* of the contact between the gold and the sulfur atoms. The Au atoms contribute  $s$  states at the Fermi level while the sulfur atoms that attach to them

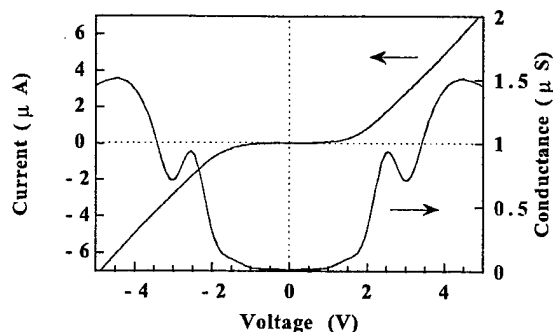


FIG. 5. Conductance of the molecule of Fig. 1 with one Au atom between the model metal surface and the sulfur for each contact as a function of the external bias applied to the metallic contacts.

contribute  $p$  states. Only the  $p$  states that are perpendicular to the electrode surfaces can couple, by symmetry, to the  $s$  states of the gold atoms, forming  $\sigma$  bonds. The  $p$  states of the sulfur atoms that are parallel to the metal surfaces do not couple to the gold  $s$  states, thus breaking the  $\pi$  scattering channel that connects the electrode to the main benzene ring. The gain in resistance is thus mainly due to the type of contacts. This conclusion is confirmed by a calculation where the single gold atoms at the contacts are replaced by aluminum atoms. For a bias of 0.01 V the resistance changes from 96 to 2.9 M $\Omega$ . The Al atoms can now contribute with  $p$  orbitals at the Fermi level that are parallel to the electrode surface and form  $\pi$  states with the  $p$  orbitals of the sulfur atoms similarly oriented. Finally, we performed a test calculation by positioning the S atom in front of the center of a triangular pad of three gold atoms on each electrode surface. This simulates a S atom on top of a Au(111) surface. The calculated resistance is nearly the same as the one for the sulfur attached to the model metal. The reason for this is that the  $s$  states of each Au atom in the pad form a state of  $s$  symmetry and two states of  $p$  symmetry parallel to the surface of the electrodes that can couple to the corresponding sulfur  $p$  state.

The above calculations show that the absolute magnitude of the current is an extremely sensitive function of the contact geometry and chemistry. For the case at hand, the discrepancy with experiment is still about an order of magnitude. There are of course additional effects that can alter the value of the current, such as temperature (hot electrons and vibrational coupling) or local disorder in the Au metal near the contacts that can produce electron localization [15]. The latter effect may arise from the breaking of the gold wire when contacts to the molecule are made [1]. We further note that the experimental measurements have an uncertainty of at least a factor of 2 [1]. Additional theoretical and experimental work is clearly needed to further clarify these issues.

In conclusion, we have simulated from first-principles the  $I$ - $V$  characteristics of a molecular device and found that the atomic-scale contact geometry and chemistry play a critical role in the absolute value of the conductance. This result sheds new light on the transport properties of molecular devices and shows that such calculations would be useful in designing devices and engineering contacts for future nanotechnology.

This work was supported in part by the National Science Foundation Grant No. DMR-98-03768, DARPA Grant No. N00014-99-1-0351, the Division of Materials Sciences, U.S. Department of Energy under Contract No. DE-AC05-96OR2264 with Lockheed Martin Energy Research Corp., and by the William A. and Nancy F. McMinn Endowment at Vanderbilt University.

- [1] M. A. Reed, C. Zhou, C. J. Muller, T. P. Burgin, and J. M. Tour, *Science* **278**, 252 (1997).
- [2] D. L. Klein, P. L. McEuen, J. E. Bowen Katari, R. Roth, and A. P. Alivisatos, *Appl. Phys. Lett.* **68**, 2574 (1996).
- [3] J. W. G. Wildoer, L. C. Venema, A. G. Rinzler, R. E. Smalley, and C. Dekker, *Nature (London)* **391**, 59 (1998); S. J. Tans, A. R. M. Verschueren, and C. Dekker, *Nature (London)* **393**, 49 (1998); S. J. Tans, M. H. Devoret, H. J. Dai, A. Thess, R. E. Smalley, L. J. Geerligs, and C. Dekker, *Nature (London)* **386**, 474 (1997).
- [4] R. Martel, T. Schmidt, H. R. Shea, T. Hertel, and Ph. Avouris, *Appl. Phys. Lett.* **73**, 2447 (1998).
- [5] M. V. Fischetti, *Phys. Rev. Lett.* **53**, 1755 (1984); M. V. Fischetti and S. E. Laux, *Phys. Rev. B* **38**, 9721 (1988).
- [6] W. B. Davis, W. A. Svec, M. A. Ratner, and M. R. Wasielewski, *Nature (London)* **396**, 60 (1998).
- [7] M. P. Samanta, W. Tian, S. Datta, J. I. Henderson, and C. P. Kubiak, *Phys. Rev. B* **53**, R7626 (1996).
- [8] J. K. Gimzewski and C. Joachim, *Science* **283**, 1683 (1999).
- [9] P. Delaney and M. Di Ventra, *Appl. Phys. Lett.* **75**, 4028 (1999); P. Delaney, M. Di Ventra, and S. T. Pantelides, *Appl. Phys. Lett.* **75**, 3787 (1999).
- [10] See, e.g., N. D. Lang, in *Solid State Physics*, edited by F. Seitz, D. Turnbull, and H. Ehrenreich (Academic, New York, 1973), Vol. 28, p. 225.
- [11] P. E. Laibinis, G. M. Whitesides, D. L. Allara, Y. T. Tao, A. N. Parikh, and R. G. Nuzzo, *J. Am. Chem. Soc.* **113**, 7152 (1991).
- [12] N. D. Lang, *Phys. Rev. B* **52**, 5335 (1995); *ibid.* **49**, 2067 (1994); N. D. Lang and Ph. Avouris, *Phys. Rev. Lett.* **81**, 3515 (1998).
- [13] W. Kohn and L. J. Sham, *Phys. Rev.* **140**, A1133 (1965); D. M. Ceperley and B. J. Alder, *Phys. Rev. Lett.* **45**, 566 (1980).
- [14] See, e.g., J. P. Perdew, K. Burke, and M. Ernzerhof, *Phys. Rev. Lett.* **77**, 3865 (1996).
- [15] P. W. Anderson, D. J. Thouless, E. Abrahams, and D. S. Fisher, *Phys. Rev. B* **22**, 3519 (1980).

# The benzene molecule as a molecular resonant-tunneling transistor

M. Di Ventra<sup>a)</sup> and S. T. Pantelides

*Department of Physics and Astronomy, Vanderbilt University, Nashville, Tennessee 37235*

N. D. Lang

*IBM Research Division, Thomas J. Watson Research Center, Yorktown Heights, New York 10598*

(Received 3 February 2000; accepted for publication 11 April 2000)

Experiments and theory have so far demonstrated that single molecules can form the core of a two-terminal device. Here we report first-principles calculations of transport through a benzene-1, 4-dithiolate molecule with a third capacitive terminal (gate). We find that the resistance of the molecule rises from its zero-gate-bias value to a value roughly equal to the quantum of resistance ( $12.9 \text{ k}\Omega$ ) when resonant tunneling through the  $\pi^*$  antibonding orbitals occurs. © 2000 American Institute of Physics. [S0003-6951(00)04023-7]

Using molecules as the active components of devices was proposed a number of years ago.<sup>1</sup> In recent years, these ideas have been revised, extended, and realized. Molecular rectification was demonstrated in 1993.<sup>2</sup> More recently, Reed *et al.* investigated the benzene-1, 4-dithiol rings as possible switching devices in molecular electronics and found their current-voltage ( $I$ - $V$ ) characteristics to be highly reproducible.<sup>3</sup> Alivisatos and co-workers<sup>4</sup> reported similar  $I$ - $V$  characteristics of semiconductor and metal nanoclusters between gold electrodes. Dekker and co-workers<sup>5</sup> reported transistor-like behavior in carbon nanotubes. Similar devices have been demonstrated by Avouris and co-workers using single- and multiwalled carbon nanotubes.<sup>6</sup> Apart from the few reports on transistor operation in nanotubes, three-terminal geometries in molecule-based devices have not been investigated because of the difficulty of realizing a gate terminal at such short length scales. However, a three-terminal device is ultimately the desired device for many of the applications of molecules in electronics. At a fixed small source-drain bias, the gate voltage must be able to amplify the current by orders of magnitude in order for the device to be a possible alternative to conventional metal-oxide-semiconductor field-effect transistors.

On the theoretical side, the transport properties of small molecules cannot be modeled by solving Boltzmann's equation as is done in conventional electronics.<sup>7</sup> Transport properties must be calculated directly from electron wave functions using a full quantum-mechanical treatment. So far, only semiempirical approaches have been employed to investigate transport in molecular systems, providing useful insights into the fundamental mechanisms.<sup>8-10</sup> We recently reported the first *ab initio* simulations of the  $I$ - $V$  characteristics of a molecule.<sup>11</sup>

In this letter we report parameter-free, fully quantum mechanical calculations of a three-terminal molecular device, namely a benzene-1, 4-dithiolate molecule attached to two electrodes and a capacitive gate. The device is formed by replacing two opposite H atoms of a benzene ring by two sulfur atoms.<sup>3,11</sup> The S atoms are then attached to two gold

electrodes. The gate is introduced as a capacitor field generated by two circular charged disks at a certain distance from each other. The axis of the capacitor is perpendicular to the transport direction. The disks are kept at a certain potential difference with the Fermi level on one disk equal to the source Fermi level (see Fig. 1). The axis of the cylindrical capacitor lies in the plane of the benzene ring.<sup>12</sup> We will show that the benzene-1, 4-dithiolate molecule exhibits amplification when a polarization field is applied perpendicular to the transport direction. In particular we show that: (a) the molecule behaves as a resonant-tunneling transistor and (b) no charging effect occurs in the molecule because the electrons do not spend enough time in the device to prevent additional charge from entering the molecule.

The benzene-1, 4-dithiolate molecule has been studied experimentally by Reed and co-workers<sup>3</sup> in a two-terminal geometry. The corresponding  $I$ - $V$  characteristics have been theoretically investigated by the present authors.<sup>11</sup> It was found that the shape of the  $I$ - $V$  characteristic is determined by the electronic structure of the molecule, as modified by the interaction with the electrodes and the presence of the external bias, and is essentially the same as that of the experimental curve.<sup>11</sup> On the other hand, the presence of single atoms at the molecule-electrode interface controls the absolute value of the current by orders of magnitude.<sup>11</sup> Amplification by employing a third terminal has not been addressed either experimentally or theoretically.

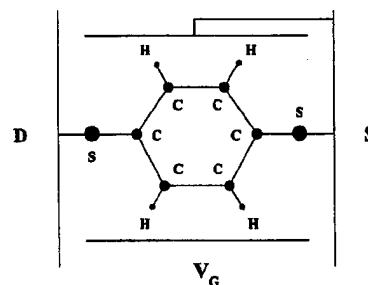


FIG. 1. Scheme of the three-terminal geometry used in the present study. The molecule is sandwiched between source and drain electrodes along the direction of electronic transport. The gate electrodes are placed perpendicular to the molecule plane. The Fermi level on one gate disk equals the source Fermi level while the other electrode is at a higher potential  $V_G$ .

<sup>a)</sup>Author to whom correspondence should be addressed; electronic mail: massimiliano.di.ventra@vanderbilt.edu

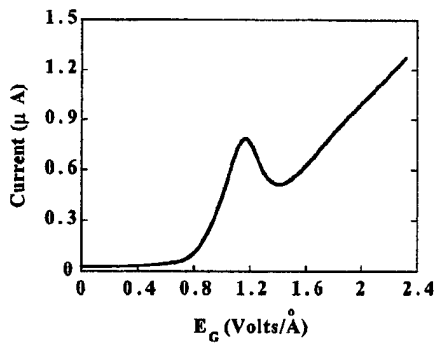


FIG. 2. Conductance of the molecule of Fig. 1 as a function of the external gate field. The source–drain bias is 0.01 V.

For the three-terminal geometry, we computed the  $I$ – $V$  characteristic using the method developed in Ref. 13 (see also Ref. 11). Since we are interested in the effects of polarization on transport, we choose for convenience the geometry for which the molecule is attached to two bare metals represented by a homogeneous electron gas or jellium model.<sup>14</sup> We assume that the molecule stands perpendicular to the metal surfaces (see Fig. 1). The electron density of the jellium electrodes is taken approximately equal to the value for metallic gold ( $r_s=3$ ). The electron wave functions are computed by solving the Lippman–Schwinger equation iteratively to self-consistency in steady state.<sup>13</sup> The current is computed from the wave functions of the electrode–molecule system in the presence of the bias and gate voltage. The differential conductance is then calculated as the derivative of the current with respect to the external bias.<sup>11</sup> Since in practical realizations of this device the gate could be of different form and size we discuss the results in terms of applied gate field along the axis of the capacitor.

The calculated  $I$ – $V$  characteristic as a function of the gate bias is shown in Fig. 2 for a source–drain voltage difference of 10 mV. After a region of constant resistance the current increases with the gate field, reaches a maximum value at 1.1 V/Å, then decreases at about 1.5 V/Å, to increase further afterward with approximately a linear dependence on the gate bias. The various features of the  $I$ – $V$  curve can be understood by looking at the density of states for different gate voltages. We recall here that the molecule has  $\pi$  bonding and  $\pi^*$  antibonding states formed by the carbon and sulfur  $p$  orbitals perpendicular to the ring plane and  $\sigma$  bonds due to the  $s$  orbitals and in-plane  $p$  orbitals of the atoms.

The initial slow rise of the conductance represents basically ohmic behavior. It is also observed experimentally for the two-terminal geometry.<sup>3,11</sup> Figure 3 (top curve) shows that the molecule has a small but relatively smooth density of states through which current can flow. The  $\pi$  bonding states lie several eV below the Fermi levels, while the  $\pi^*$  antibonding states are nearly 1 eV above the Fermi levels.

After the initial increase of the current with increasing gate bias, a first conductance peak and subsequent valley are observed. The peak and the valley are due to resonant tunneling through  $\pi^*$  antibonding states. The gate field couples  $\pi^*$  states with the continuum of states at higher energy. Since the gate field is parallel to the electrode surfaces, only the odd (with respect to an axis parallel to the surface of the

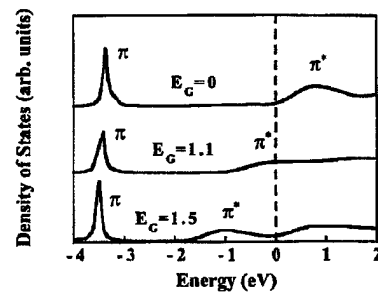


FIG. 3. Difference between the density of states of the two semi-infinite electrodes with and without the benzene-1,4-dithiolate molecule in between, for three different gate fields  $E_G$  (in units of V/Å). The left Fermi level has been chosen as the zero of energy. The right Fermi level is at 10 mV.

electrodes and on the molecule plane) component of the continuum states couples to the  $\pi^*$  states.<sup>15</sup> This is the equivalent of the usual quadratic Stark shift effect in atoms and molecules.<sup>16</sup> The effect is less pronounced for the  $\pi$  states because they are much more separated in energy from the continuum states of higher energy than are the  $\pi^*$  orbitals. The antibonding states thus shift in energy and eventually enter into resonance with the states between the right and left Fermi levels, separated by 10 meV (middle curve of Fig. 3). Increasing the bias further (bottom curve of Fig. 3), the resonant-tunneling condition is lost and a valley in the  $I$ – $V$  characteristic is observed. Finally, as the gate bias is increased further, the current starts to increase approximately linearly with the gate bias. This can be readily understood within the Kubo–Greenwood formalism:<sup>17</sup> increasing the gate bias, quasifree electron states with increasing energy enter the window of energy between the right and left Fermi levels and can thus contribute to transport. Assuming the electronic effective masses are approximately the same at different energies, the conductivity (and thus the current since the source–drain bias is only 10 mV) increases with the square of the density of states at the energy of interest.<sup>17</sup> For the electron gas of these quasifree states, the density of states can be assumed to vary as the square root of the single particle energy, and thus the current varies almost linearly with the external gate bias.

The peak-to-valley ratio of the present system is 1.4, which is probably so small that it would be washed out by the vibrational coupling with the modes of the molecule. This has already been argued in the two-terminal geometry case:<sup>11</sup> the peak-to-valley ratios observed experimentally in the present system are considerably smaller than theoretically predicted.<sup>3,11</sup>

The value of the gate field at which resonant tunneling occurs ( $\approx 1$  V/Å) seems slightly high for a molecule with a nominal length of 8 Å. Two observations are however in order: (i) we found in previous work<sup>11</sup> that the theoretical peak of transmission due to  $\pi^*$  antibonding states occurs at higher external bias than the experimental one. This discrepancy is due in part to known limitations of the local density approximation.<sup>18</sup> (ii) In a practical realization of the device, the capacitance field would certainly leak into the source and drain electrodes, providing a pocket of electrons with higher kinetic energy to tunnel, thus reducing the gate bias value at which resonance occurs. Both remarks suggest that resonant tunneling and amplification can occur at lower gate field.

The resistance at zero gate bias is about 360 k $\Omega$ . At 1.1 V/Å its value changes to 12.7 k $\Omega$ . The peak value is close to the single-channel resistance of 12.9 k $\Omega$  (spin included). At resonance, the lowest  $\pi^*$  antibonding state is exactly in the narrow window of energy defined by the right and left Fermi levels, providing a single channel for electrons to tunnel. We stress that this value could not be obtained without a self-consistent approach: the transmission coefficient of the channel is not necessarily unity,<sup>10</sup> and depends on how the electronic charge redistributes in the molecule and at the contacts. The amplification (from the zero gate field to the gate field at which resonant tunneling occurs) is more than 1 order of magnitude. The measured resistances of this molecule<sup>3</sup> are in fact much larger than the theoretical values.<sup>11</sup> We have shown that these resistances are partly due to the chemistry and geometry of the contacts and do not affect considerably the electronic structure of the molecule-electrode system.<sup>11</sup> Much larger amplification should, therefore, be obtained in a practical implementation of the device, since the value of the resistance when resonant tunneling occurs is close to (even if not exactly the same as) the single-channel resistance.

We conclude this letter by suggesting that no sizeable charging effect should be observed in the  $I$ - $V$  characteristics for the present system. Indeed, the electrons do not spend enough time in the device to charge it. This time can be estimated by calculating the delay time an electron spends in the scattering region whatever the outcome of the scattering event (the electron either transmitted or reflected),<sup>19</sup> and is related to the difference of density of states  $\Delta D(E)$  of the two semi-infinite electrodes with and without the benzene-1,4-dithiolate molecule in between as  $\tau = \hbar \pi \Delta D(E)$ . At small gate fields (where Coulomb blockade could potentially be observed) the delay time is about 2 fs. In this time, only a charge of  $0.04|e|$  is present in the molecular region between the source and drain electrodes and the energy region between the right and left Fermi levels.<sup>20</sup> Due to the short delay time and the small extra charge present in the molecular region, we suggest that transport occurs by tunneling and that no Coulomb blockade is present.

This work was supported in part by Grant No. MDA972-98-1-0007 from DARPA, and by the William A. and Nancy F. McMinn Endowment at Vanderbilt University. The calculations have been performed on the IBM SP2 at the NPACI in San Diego.

- <sup>1</sup> See, e.g., A. Aviram and M. A. Ratner, *Chem. Phys. Lett.* **29**, 277 (1974).
- <sup>2</sup> D. H. Waldeck and D. N. Beratan, *Science* **261**, 576 (1993); A. S. Martin, J. R. Sambles, and G. J. Ashwell, *Phys. Rev. Lett.* **70**, 218 (1993).
- <sup>3</sup> M. A. Reed, C. Zhou, C. J. Muller, T. P. Burgin, and J. M. Tour, *Science* **278**, 252 (1997); J. Chen, M. A. Reed, A. M. Rawlett, and J. M. Tour, *ibid.* **286**, 1550 (1999).
- <sup>4</sup> D. L. Klein, P. L. McEuen, J. E. Bowen Katari, R. Roth, and A. P. Alivisatos, *Appl. Phys. Lett.* **68**, 2574 (1996).
- <sup>5</sup> J. W. G. Wildoer, L. C. Venema, A. G. Rinzler, R. E. Smalley, and C. Dekker, *Nature (London)* **391**, 59 (1998).
- <sup>6</sup> R. Martel, T. Schmidt, H. R. Shea, T. Hertel, and Ph. Avouris, *Appl. Phys. Lett.* **73**, 2447 (1998).
- <sup>7</sup> M. V. Fischetti, *Phys. Rev. Lett.* **53**, 1755 (1984).
- <sup>8</sup> W. B. Davis, W. A. Svec, M. A. Ratner, and M. R. Wasielewski, *Nature (London)* **396**, 60 (1998).
- <sup>9</sup> M. P. Samanta, W. Tian, S. Datta, J. I. Henderson, and C. P. Kubiak, *Phys. Rev. B* **53**, R7626 (1996).
- <sup>10</sup> P. Delaney, M. Di Ventra, and S. T. Pantelides, *Appl. Phys. Lett.* **75**, 3787 (1999); P. Delaney and M. Di Ventra, *ibid.* **75**, 4028 (1999).
- <sup>11</sup> M. Di Ventra, S. T. Pantelides, and N. D. Lang, *Phys. Rev. Lett.* **84**, 979 (2000).
- <sup>12</sup> The disks have radius 4 Å and are kept at a distance of 7.4 Å. In this way, the capacitance field covers the entire region of the molecule without leakage into the source and drain electrodes.
- <sup>13</sup> N. D. Lang, *Phys. Rev. B* **52**, 5335 (1995); M. Di Ventra, S. T. Pantelides, and N. D. Lang (unpublished).
- <sup>14</sup> See, e.g., N. D. Lang, in *Solid State Physics*, edited by F. Seitz, D. Turnbull, and H. Ehrenreich (Academic, New York, 1973), Vol. 28, p. 225.
- <sup>15</sup> The  $\pi$  and  $\pi^*$  states are formed by  $p$  orbitals perpendicular to the molecule plane. These states are thus even with respect to the gate field direction.
- <sup>16</sup> See, e.g., B. H. Bransden and C. J. Joachain, in *Physics of Atoms and Molecules* (Longman Group Limited, New York, 1983), p. 377.
- <sup>17</sup> M. Di Ventra and S. T. Pantelides, *Phys. Rev. B* **59**, R5320 (1999).
- <sup>18</sup> See, e.g., J. P. Perdew, K. Burke, and M. Ernzerhof, *Phys. Rev. Lett.* **77**, 3865 (1996).
- <sup>19</sup> M. Sassoli de Bianchi and M. Di Ventra, *J. Math. Phys.* **36**, 1753 (1995).
- <sup>20</sup> This charge has been calculated as the difference between the charge of the total system and the charge of the bare electrodes, integrating between the right and left Fermi levels in a volume of  $8.3 \times 8.3 \times 11.9 \text{ \AA}^3$ . This volume comprises most of the potential induced by the presence of the molecule.

## Hellmann-Feynman theorem and the definition of forces in quantum time-dependent and transport problems

Massimiliano Di Ventra

*Department of Physics and Astronomy, Vanderbilt University, Nashville, Tennessee 37235*

Sokrates T. Pantelides

*Department of Physics and Astronomy, Vanderbilt University, Nashville, Tennessee 37235  
and Solid State Division, Oak Ridge National Laboratory, Oak Ridge, Tennessee 37831*

(Received 16 August 1999)

The conventional Hellmann-Feynman theorem for the definition of forces on nuclei is not directly applicable to quantum time-dependent and transport problems. We present a rigorous derivation of a general Hellmann-Feynman-like theorem that applies to all quantum mechanical systems and reduces to well-known results for ground-state problems. It provides a rigorous definition of forces in time-dependent and transport problems. Explicit forms of Pulay-like forces are derived and the conditions for them to be zero are identified. A practical scheme for *ab initio* calculations of current-induced forces is described and the study of the transfer of a Si atom between two electrodes is presented as an example.

### I. INTRODUCTION

The Hellmann-Feynman (HF) theorem<sup>1</sup> has been a key ingredient of the quantum mechanical treatment of forces acting on nuclei in molecules and solids. In turn, these forces are the key ingredient of *ab initio* calculations of atomic-scale structure and dynamics in materials physics, chemistry, and molecular biology.<sup>2-8</sup> In such calculations, the electron system is kept in its instantaneous ground state, for which the traditional formulations of the HF theorem apply. For example, for several decades, theoretical investigations of molecules and chemical reactions have relied on potential energy surfaces computed in this fashion. In the last two decades, a similar approach has been the basis for calculations in solids, e.g., surface reconstruction, phase transformations, defect configurations, and defect reactions. In more recent years, fully dynamical calculations (e.g., the Car-Parrinello method<sup>2,3</sup>) generally assume the electron system remains in its instantaneous ground state.

The conventional formulations of the HF theorem,<sup>2-8</sup> however, do not apply to two important classes of problems in which the electron system is not in the ground state. Both these classes are emerging frontiers for *ab initio* quantum mechanical calculations.

(a) Molecules and solids in *time-dependent* external fields, e.g., radiation. In such systems, the external field generally induces electronic excitations and nuclear motions. The advent of powerful free-electron lasers and of tabletop lasers that deliver intense ultrashort pulses has renewed interest in the photodissociation of molecules and other ultrafast reactions,<sup>9</sup> the generation of high harmonics, including x rays, from atoms in intense infrared pulses,<sup>10,11</sup> the photo-induced desorption of atoms and molecules from solid surfaces,<sup>12</sup> and other phenomena, especially in the nonlinear regime.

(b) *Transport* in nanostructures and molecules. The fabrication of electronic devices using nanoparticles or molecules<sup>13,14</sup> and the use of a scanning-tunneling micro-

scope to create atomic-scale structures on crystal surfaces<sup>15</sup> represent transport problems for which the traditional Boltzmann equation approach does not apply.<sup>16</sup> Fully quantum mechanical calculations of transport properties are needed, including calculations of current-induced atomic rearrangements. The macroscopic manifestation of the latter, namely electromigration, has remained an open question through the years<sup>17,18</sup> and is ripe for direct first-principles calculations.

For both classes of problems, the conventional formulations of the HF theorem and its generalizations are not applicable and the proper definition of the force on nuclei has remained unsettled.<sup>10,18-20</sup> Some attempts to extend the HF theorem to nonstationary states have been proposed<sup>22</sup> but, as we show later in the paper, they rely on an incorrect physical assumption.

In this paper, we will first give a concise statement of the HF theorem for eigenstate and variational ground-state problems as a point of reference and identify the precise obstacles that have left the problem unsettled for the time-dependent and transport problems. We will then present a general form of the HF theorem that is applicable to all quantum mechanical systems with square-integrable wave functions. The proper definition of forces and their implementation in practical calculations will then become clear. We will show that this general theorem and its practical implementations reduce to the classic results for systems in the ground state. An example will be provided for the forces acting on a Si atom between two electrodes when steady-state current flows.

### II. HF THEOREM FOR GROUND STATE

Throughout this paper we will present derivations using a many-body Hamiltonian  $H$  and many-body square-integrable wave functions  $\Psi$  for a system of nuclei and electrons without any particular approximations. Analogous derivations can easily be formulated using specific approaches to the many-body problem such as Hartree-Fock or density-

functional theory (DFT). The explicit equations for DFT are given in the Appendix.

Given the eigenvalue problem

$$H\Psi = E\Psi, \quad (1)$$

where  $H$  depends parametrically on a quantity  $\lambda$  and  $\Psi$  is square-integrable, it is straightforward to show by direct differentiation that

$$\frac{dE}{d\lambda} = \left\langle \Psi \left| \frac{\partial H}{\partial \lambda} \right| \Psi \right\rangle / \langle \Psi | \Psi \rangle + \left[ \left\langle \Psi \left| H - E \right| \frac{\partial \Psi}{\partial \lambda} \right\rangle + \left\langle \frac{\partial \Psi}{\partial \lambda} \left| H - E \right| \Psi \right\rangle \right] / \langle \Psi | \Psi \rangle. \quad (2)$$

In view of Eq. (1), Eq. (2) reduces to

$$\frac{dE}{d\lambda} = \left\langle \Psi \left| \frac{\partial H}{\partial \lambda} \right| \Psi \right\rangle / \langle \Psi | \Psi \rangle. \quad (3)$$

This last equation represents the HF theorem for *exact* eigenstates. If the quantity  $\lambda$  is a given degree of freedom of the system, then the quantity  $-dE/d\lambda$  given by Eq. (3) can be interpreted as the generalized force associated with it. In particular, if the nuclei (or ions) are treated as classical particles and  $\lambda$  is the position vector of a nucleus, then  $-dE/d\lambda$  is the classical force on that nucleus.

The practical importance of the HF theorem is that energy derivatives are difficult to compute numerically, whereas the expression on the right in Eq. (3), the negative of which is known as the HF force, can be computed efficiently. However, it was recognized by early computational work using atom-centered basis functions that the HF force gave manifestly wrong results.<sup>5</sup> The origin of the problem is most succinctly illustrated by noting that, for a variational calculation of the ground-state energy  $E$ , when  $\Psi$  is expanded in terms of a *finite basis set*, one no longer has Eq. (1) but the more restrictive

$$\langle \Psi | H - E | \Psi \rangle = 0, \quad (4)$$

where  $E$  and  $\Psi$  now are the variational energy and wave function, respectively. Equation (4) is now a *matrix equation*. As a result, the second term in Eq. (2) is no longer zero.

Two approaches have been pursued in the literature:

(a) One requires that the basis set is such that the extra term in Eq. (2) is identically zero. This requirement, known as Hurley's condition,<sup>21</sup> is satisfied if the basis functions do not depend on  $\lambda$  (e.g., when the parameters  $\lambda$  are nuclear position vectors; such sets are known as "floating sets" in quantum chemistry; in solid state applications, the commonly used plane waves are such a set). The condition is also satisfied if the derivatives of the basis functions with respect to  $\lambda$  are themselves part of the basis set.<sup>4</sup> In such a case, the original HF theorem is satisfied. In order to prove these statements, one writes in matrix notation

$$\Psi = C\chi, \quad (5)$$

where  $\{\chi\}$  is the basis set and  $C$  the expansion coefficients. From the stationarity principle,  $\delta E / \delta \Psi = 0$ , we get  $\delta E / \delta C = 0$ , so that only the derivatives  $d\chi/d\lambda$  survive in  $\partial \Psi / \partial \lambda$  in Eq. (2).

(b) One works with the full Eq. (2). The usual interpretation of this equation is that  $-dE/d\lambda$  represents the exact force, the negative of the first term on the right is the HF force, and the negative of the last term is a correction term often referred to as the Pulay force.<sup>5</sup> This interpretation was backed by the fact that, as we already mentioned, attempts to use the HF force alone with atom-centered basis orbitals gave manifestly wrong results.<sup>5</sup> The Pulay force is routinely included in calculations using atom-centered basis functions and is in fact needed to produce realistic results. It is viewed as a correction to the HF force needed to make the calculation accurate to second order.<sup>5,6</sup>

From this perspective, it is clear why the problem of forces in time-dependent and transport problems remains unsolved: it is not obvious that, in these cases, one can meaningfully define a force in terms of an energy derivative. Moreover, it was recognized that there is no HF theorem that would connect the energy derivative to the practical HF force.<sup>18</sup> It has been argued, however, that, even in the absence of a HF theorem, the HF force [right-hand side of Eq. (3)] remains the correct quantum mechanical force for time-dependent and transport problems because of the Ehrenfest theorem that relates this force to the time derivative of the expectation value of the (generalized) momentum operator.<sup>10,18</sup> This assertion is appealing, but has not been tested and *runs contrary to the established fact* that, for variational ground-state calculations using atom-centered basis sets, the HF force alone is inadequate and the corrections introduced by the Pulay terms are not negligible.

### III. TIME-DEPENDENT PROBLEM

We have now laid the groundwork to present a rigorous formulation of forces for all quantum mechanical problems. The first step is to recognize that the only correct and most general quantum mechanical definition of a force is the expectation value of the time derivative of the momentum operator.<sup>23</sup> For the most general, time-dependent quantum mechanical problem defined by

$$H\Phi = i \frac{\partial}{\partial t} \Phi \quad (6)$$

(we use units such that  $\hbar = 1$  and we use  $\Phi$  to denote time-dependent wave functions), the force for a given degree of freedom  $\lambda$  is defined by<sup>23</sup>

$$F = -i \frac{d}{dt} \left\langle \Phi \left| \frac{\partial}{\partial \lambda} \right| \Phi \right\rangle / \langle \Phi | \Phi \rangle. \quad (7)$$

If  $\lambda$  is the position vector of a given nucleus, then the force in Eq. (7) is simply the time derivative of the expectation value of the momentum operator of that nucleus.

If we specialize this definition to time-independent problems for which

$$\Phi(t) = e^{-iEt} \Psi, \quad (8)$$

we get immediately

$$F = - \frac{dE}{d\lambda}. \quad (9)$$

Two most important observations are in order: first, *the reduction of the force definition to the energy-derivative form is only possible for time-independent problems*; and second, for time-independent problems, this reduction is valid for both exact wave functions and wave functions expressed in terms of a finite basis set. These observations validate rigorously the long-standing assumption that, for time-independent eigenstate problems, the force can be defined in terms of the derivative of the energy. They also make clear the fact that, for time-dependent problems, the rigorous definition of the force is Eq. (7).

We now address the issue of connecting the rigorous force definition to the HF force in the general case. By direct differentiation of the definition (7) and use of Eq. (6), it is straightforward to show that, *for exact wave functions*

$$i \frac{d}{dt} \left\langle \Phi \left| \frac{\partial}{\partial \lambda} \right| \Phi \right\rangle = \left\langle \Phi \left| \frac{\partial H}{\partial \lambda} \right| \Phi \right\rangle. \quad (10)$$

This is the usual Ehrenfest theorem that can be found in textbooks.<sup>23</sup> In view of Eqs. (7) and (9), we see immediately that for time-independent problems, the Ehrenfest theorem reduces to Eq. (3), namely the HF theorem. In fact, the Ehrenfest theorem has been referred to as the time-dependent version of the HF theorem.<sup>19</sup> One observation is crucial, however. The Ehrenfest theorem [Eq. (10)] is only valid for *exact* wave functions. When the wave functions are expanded in terms of a finite basis set, as in most computational work, one must derive the corresponding *finite-set Ehrenfest-like theorem*. We note that, for finite basis sets, we no longer have Eq. (6), but the more restrictive

$$\left\langle \Phi \left| H - i \frac{\partial}{\partial t} \right| \Phi \right\rangle = 0, \quad (11)$$

which is a matrix equation. By direct differentiation and some algebraic manipulation, we then get *the finite-set Ehrenfest theorem*:

$$\begin{aligned} i \frac{d}{dt} \left\langle \Phi \left| \frac{\partial}{\partial \lambda} \right| \Phi \right\rangle &= \left\langle \Phi \left| \frac{\partial H}{\partial \lambda} \right| \Phi \right\rangle + \left\langle \frac{\partial \Phi}{\partial \lambda} \left| H - i \frac{\partial}{\partial t} \right| \Phi \right\rangle \\ &+ \left\langle \Phi \left| H + i \frac{\partial}{\partial t} \right| \frac{\partial \Phi}{\partial \lambda} \right\rangle. \end{aligned} \quad (12)$$

This is the central result of this paper and represents the most general form of an HF-like theorem that is applicable to all systems and allows a correct and unambiguous definition of forces for practical implementation. Note that this approximate form of the Ehrenfest theorem reduces to the exact form, Eq. (10), when the basis is complete, simply because Eq. (6) and its complex conjugate are then exact. When we specialize the finite-set theorem of Eq. (12) to the time-independent case, we immediately get Eq. (2). Thus, as is the case for time-independent problems, we find that when the appropriate form of the Ehrenfest theorem is used, the HF force is *not necessarily* the correct definition of force. The extra terms in Eq. (12) are the analog of the Pulay forces for the time-dependent problem. The Pulay forces can again be made zero by an appropriate choice of a basis set, as in the time-independent Hurley's condition. In other words, the Pulay forces are zero if the basis functions do not depend on  $\lambda$

or if their derivatives are also members of the set. In order to prove this statement, it is necessary to invoke the fact that in time-dependent problems, the action  $S$  defined by

$$S = \int_{t_0}^t \left\langle \Phi \left| H - i \frac{\partial}{\partial t} \right| \Phi \right\rangle dt \quad (13)$$

is stationary for a given  $\Phi$ , namely  $\delta S / \delta \Phi = 0$ , so that when we expand  $\Phi = C\chi$ , we have  $\delta S / \delta C = 0$ . For plane waves and "floating sets," the Pulay-like terms are again zero and the HF force is the exact force. Otherwise, the Pulay-like terms must be included. Note also that, in the most general case, stationarity of the action does not imply a minimum principle, indicating that the accuracy of the results is very sensitive to the choice of the approximate wave functions employed.<sup>10</sup>

We can now compare directly the above results with prior literature. As we already remarked, the assertion by Gross *et al.*<sup>10</sup> regarding the use of the HF force is rigorously correct in the limit of a complete basis set and remains valid when the generalized Hurley condition is satisfied, as discussed previously (see also the Appendix). Otherwise, Pulay-like forces must be included. It is also clear from the above analysis why the Bala *et al.* results<sup>22</sup> are not correct: the correct definition of the force in quantum mechanics is the time derivative of the expectation value of the momentum operator and *not* the  $\lambda$  derivative of the expectation value of the Hamiltonian on time-dependent wave functions.

#### IV. STEADY-STATE TRANSPORT PROBLEM

We turn now to the transport problem. The general formalism above is actually valid for all problems describable by square-integrable wave functions. The only question, therefore, is one of normalization of wave functions. In the eigenstate and variational ground-state problems one deals with either finite systems (molecules, clusters) or with infinite solids for which square-integrability is attained through periodic Born-von Kármán boundary conditions. For transport problems, square-integrability is ensured if one describes the complete circuit, including, e.g., the battery or generator. In the most general case of time-dependent power source, the above time-dependent formalism is completely valid. For practical calculations, however, one normally treats a system, say a device  $D$ , in contact with electrodes that act as reservoirs of electrons and serve merely as boundary conditions for the wave function of  $D$ . Square integrability can then be assured by constructing new many-electron wave functions from wave packets centered at individual one-electron energies.

For time-independent direct-current (dc) *steady-state* transport, the most general form of the many-body wave function of the system  $D$  is again as in Eq. (8), where now  $E$  is a phase factor with units of energy. Using this form in Eq. (13) we find that the action becomes

$$S = \langle \Phi | H - E | \Phi \rangle (t - t_0). \quad (14)$$

The stationarity of the action<sup>10</sup> now yields

$$\delta \langle \Phi | H - E | \Phi \rangle = 0. \quad (15)$$

The equation above shows that the dc transport problem can be rigorously mapped onto a variational problem where  $\langle \Psi | H | \Psi \rangle / \langle \Psi | \Psi \rangle$  is the steady-state energy of the system.

It differs from the ground-state problem only in the form of boundary conditions (closed versus open). Again, for plane waves and "floating sets," the HF force represents the total force whereas for other sets Pulay-like forces must be included as in Eq. (2).

So far our derivations were carried out for the many-body Hamiltonian  $H$  and wave functions  $\Psi$  or  $\Phi$ . For practical implementations, one normally separates the nuclear and electronic degrees of freedom and treats the nuclei as classical particles (see the Appendix). The Hamiltonian then depends parametrically on the nuclear position vectors, which can be treated as  $\lambda$ 's in the present theory. The corresponding forces are the classical forces on the nuclei. For ground-state and time-dependent problems the general theory above can then easily be cast within the respective Hartree-Fock or density-functional formulations of the many-electron problem. For dc transport, Eq. (15) allows us to conclude that ground-state density-functional theory is again applicable with the steady-state energy of the system  $D$  playing the role of the ground-state energy. This result provides formal justification for the use of one-electron theories for transport calculations. We note, however, that for the transport problem, a practical implementation is still lacking for realistic systems. We conclude the paper by summarizing the main elements of such a practical scheme.

We consider the system  $D$  and two (or more) electrodes ( $R$  and  $L$  for right and left). Each of these systems can be treated separately by density functional theory. Let us designate the corresponding *single-particle* Hamiltonians by  $H_D$ ,  $H_R$ , and  $H_L$ . The coupling between the system and the electrodes can then be included by defining the total single-particle Hamiltonian as

$$H = H_D + H_L + H_R + H_{LC}^I + H_{RC}^I, \quad (16)$$

where  $H_{LC}^I$  and  $H_{RC}^I$  are Hermitian operators to be determined. Only the Hamiltonians  $H_{LC}^I$ ,  $H_{RC}^I$ , and  $H_D$  are assumed to depend on the position of the atoms. The external electric field is introduced by requiring that, far from the system, the Fermi-level difference between the left and right electrodes is equal to the desired value.<sup>20</sup> As we showed above, the steady-state energy of the system is defined in terms of the ground-state energy functional evaluated with the new wave functions obeying the transport boundary conditions.<sup>24</sup>

The most effective approach to a self-consistent determination of  $H_{LC}^I$ ,  $H_{RC}^I$ , and  $\Psi$  is the Green's function method, where  $H_{LC}^I + H_{RC}^I + H_D$  is viewed as the perturbation to the bare electrodes. So far this problem has been addressed *without considering the problem of forces by several authors*.<sup>20,25,26</sup> A practical scheme has been developed by Lang<sup>20</sup> by assuming that the electrodes are described by "jellium," namely, a homogeneous electron gas with a smeared-out compensating positive background. Formulations using real metals are *not* well-suited for practical calculations because of ambiguities in ordering the wave functions by energy.<sup>26</sup> We propose, therefore, the following scheme for practical calculations, including force calcula-

tions: The electrodes can be approximated by jellium only far from the system-electrode junctions so that the electrode wave functions can be easily ordered by the asymptotic behavior as plane waves. We anticipate that only a few layers of metal atoms would be needed attached to jellium continua. For the actual calculations, the metal layers are viewed as part of the system in the cavity between jellium electrodes. Lang's formalism can then be used to determine  $H$  and  $\Psi$  self-consistently, and current-induced forces on atoms can be computed as in variational problems in accordance with the theorem proven in the present paper.<sup>27</sup> The spurious resistance introduced by the jellium-metal interface can be calculated separately and subtracted. We note that the discrete as well as the continuous spectrum of the whole system can be included in the formalism above in a straightforward way. This is of extreme importance in such phenomena such as electromigration, where the contributions coming from the continuous and discrete parts of the spectrum are of the same order of magnitude.<sup>18</sup>

We conclude with a practical example applying the formulation above to the problem of a Si atom between two electrodes.<sup>28</sup> The two electrodes are kept at a distance of 4.5 Å. An external bias is applied between the right and left electrode, the left electrode being positive with respect to the right electrode. The spectrum of the present system has a discrete and a continuum component. For the single-particle wave functions in the discrete part of the spectrum  $\psi_i$ , square-integrability is satisfied because the  $\psi_i$ 's are localized. For each energy in the continuum we build square-integrable wave functions  $\tilde{\psi}$  in an energy region  $\Delta$ , as we stated above:

$$\tilde{\psi} = A \int_{\Delta} dE \psi, \quad (17)$$

where  $A$  is a normalization constant and  $\psi$ 's are single-particle wave functions in the continuum. As in Ref. 29 we choose plane waves to represent the Hilbert space.<sup>30</sup> According to Eq. (2), the Pulay-like terms are thus identically zero. The force  $\mathbf{F}$  acting on the atom at position  $\mathbf{R}$  due to the electron distribution as modified by the external bias is thus

$$\mathbf{F} = \sum_i \left\langle \psi_i \left| \frac{\partial H}{\partial \mathbf{R}} \right| \psi_i \right\rangle + \lim_{\Delta \rightarrow 0} \int_{\sigma} dE \left\langle \tilde{\psi} \left| \frac{\partial H}{\partial \mathbf{R}} \right| \tilde{\psi} \right\rangle. \quad (18)$$

The sum and integral in Eq. (18) include spin variable too. In the present case, no ion-ion interaction must be included. The continuum integration  $\sigma$  covers the part of the spectrum occupied by the electrons at a given bias: at  $T=0$ , from the bottom of the conduction band on the left to the quasi-Fermi-level on the right.<sup>31</sup>

In the case at hand, the force is directed along the direction perpendicular to the electrode surfaces. The results are plotted in Fig. 1 for two different external bias conditions: 0 V and 3 V.<sup>28</sup> At zero bias the Si atom has two stable and one metastable configurations. The stable configurations correspond to the atom at about 1.2 Å from the two metals. The metastable configuration corresponds to the atom between the two electrodes. The stable configurations at zero bias coincide exactly with the equilibrium positions obtainable from standard density-functional total-energy calculations.<sup>32</sup>

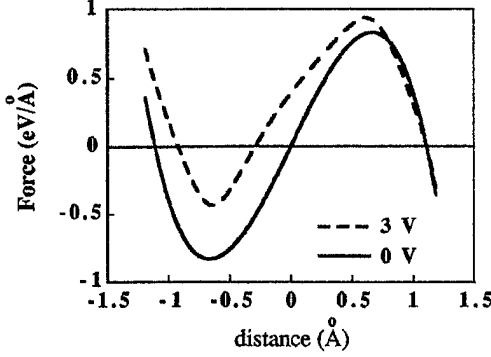


FIG. 1. Force on a single Si atom between two electrodes separated by 4.5 Å for two different external biases: 0 V and 3 V. Positive force pushes the atom to the right. Zero distance corresponds to the atom between the two electrodes.

The work necessary to bring the atom from one electrode to the other can be calculated from the curves in Fig. 1 as the integral between the metastable and stable configurations. At zero bias the work done is about 0.5 eV. Applying 3 V across the electrodes (the left electrode is at the higher bias), the stable positions shift slightly towards the right electrode due to a transfer of charge on the left electrode. Finally, the activation barrier to bring the atom from its left stable configuration to the new metastable position decreases to about 0.1 eV. The atom is essentially free to jump to the right electrode when the bias is 3 V.

## V. CONCLUSIONS

We presented a general HF theorem that applies to all quantum mechanical systems and allows a rigorous definition of forces in all cases, including those where a finite basis set is used to represent the system wave functions. In the latter case, Pulay-like forces arise that can be set to zero with a particular choice of the basis functions. We also presented a practical scheme for transport calculations in nanostructures that includes current-induced forces on atoms. The latter scheme is particularly important nowadays to provide valuable insight into current effects on molecular devices.

## ACKNOWLEDGMENTS

We thank N.D. Lang for providing us with his code that solves the Lippman-Schwinger equation iteratively to self-consistency in steady state. The code has been modified by the present authors to include forces on atoms according to the scheme described in the text. This work was supported in part by the National Science Foundation Grant No. DMR-98-03768, DARPA Grant No. N00014-99-1-0351, and the Division of Materials Sciences, U.S. Department of Energy under Contract No. DE-AC05-96OR2264 with Lockheed Martin Energy Research Corp., and we thank William A. and Nancy F. McMinn Vanderbilt University for financial support.

## APPENDIX: FORCES IN DFT

We explicitly write in this appendix the expressions of the HF forces in DFT. We recall that the total energy of a many-

electron system with charge density  $n(\mathbf{r})$  in an external potential  $V(\mathbf{r})$  can be written as a functional of the density<sup>33</sup>

$$E[n] = T_s[n] + \int V(\mathbf{r})n(\mathbf{r})d\mathbf{r} + \frac{e^2}{2} \iint \frac{n(\mathbf{r})n(\mathbf{r}')}{|\mathbf{r}-\mathbf{r}'|} d\mathbf{r}d\mathbf{r}' + E_{xc}[n]. \quad (\text{A1})$$

$T_s$  is the kinetic energy of noninteracting electrons, and  $E_{xc}[n]$  is the exchange-correlation energy. The quantum mechanical problem is solved with variational wave functions. According to Eq. (3), the electronic contribution to the force acting on a nuclear degree of freedom  $\lambda$  is thus

$$F = -\frac{dE[n]}{d\lambda} = -\int \frac{\partial V(\mathbf{r})}{\partial \lambda} n(\mathbf{r})d\mathbf{r} - \int \frac{\delta E(\mathbf{r})}{\delta n} \frac{\partial n(\mathbf{r})}{\partial \lambda} d\mathbf{r}, \quad (\text{A2})$$

where  $\delta E(\mathbf{r})/\delta n$  is the variation of the functional with respect to the density. The first term in Eq. (A2) is the HF force, while the second is the Pulay-like term. If the ionic potentials are spherically symmetric and their non-Coulomb parts do not overlap, a classical electrostatic term, representing the ion-ion interaction, must be added to Eq. (A2) to obtain the total force on nuclei.

In time-dependent DFT, Eq. (6) decouples into a set of coupled equations for all electrons  $\psi_i$  and nuclei  $\phi_i$  (with charge  $Z_i$ ) under external time-dependent potentials  $V(\mathbf{r}, t)$  and  $V(\lambda, t)$ , respectively,

$$i\frac{\partial}{\partial t} \psi_i(\mathbf{r}, t) = \left( T_s[n] + V(\mathbf{r}, t) + \int \frac{n(\mathbf{r}')}{|\mathbf{r}-\mathbf{r}'|} d\mathbf{r}' + E_{xc}[n] \right) \psi_i(\mathbf{r}, t), \quad (\text{A3})$$

$$i\frac{\partial}{\partial t} \phi_i(\lambda, t) = \left[ T_\lambda + V(\lambda, t) - Z_i \times \int \frac{n(\mathbf{r}')}{|\mathbf{r}-\mathbf{r}'|} d\mathbf{r}' + E_{xc}[n](\lambda, t) \right] \phi_i(\lambda, t),$$

where  $T_\lambda$  is the nuclei kinetic energy and  $E_{xc}[n](\lambda, t)$  is the nuclear exchange-correlation potential. Note that, in our notation,  $V(\mathbf{r}, t)$  and  $V(\lambda, t)$  contain the electron-ion and ion-ion interactions, respectively. Assuming the nuclei as classical particles with nuclear distribution  $n_i(\lambda, t) = |\phi_i(\lambda, t)|^2 = \delta(\lambda - \lambda_i(t))$  and applying Eq. (12) to the nuclear motion, the force on the nuclei is

$$F_i(t) = -\nabla_{\lambda_i(t)} V(\lambda, t) - Z_i \times \int \frac{n(\mathbf{r}')}{|\lambda_i(t) - \mathbf{r}'|^2} + Z_i \int \frac{\nabla_{\lambda_i(t)} n(\mathbf{r}')}{|\lambda_i(t) - \mathbf{r}'|}. \quad (\text{A4})$$

The last term of Eq. (A4) is the Pulay-like force in time-dependent DFT.

- <sup>1</sup>H. Hellmann, *Einführung in die Quantenchemie* (Franz Deuticke, Leipzig, 1937), Sec. 54; R.P. Feynmann, *Phys. Rev.* **56**, 340 (1939).
- <sup>2</sup>R. Car and M. Parrinello, *Phys. Rev. Lett.* **55**, 2471 (1985).
- <sup>3</sup>M.C. Payne, M.P. Teter, D.C. Allan, T.A. Arias, and J.D. Joannopoulos, *Rev. Mod. Phys.* **64**, 1045 (1992).
- <sup>4</sup>H. Nakatsuji, T. Hayakawa, and M. Hada, *Chem. Phys. Lett.* **80**, 94 (1981).
- <sup>5</sup>P. Pulay, in *Modern Theoretical Chemistry*, edited by H.F. Schaefer (Plenum, New York, 1977), Vol. 4.
- <sup>6</sup>M. Scheffler, J.P. Vigneron, and G.B. Bachelet, *Phys. Rev. B* **31**, 6541 (1985).
- <sup>7</sup>P. Bendt and A. Zunger, *Phys. Rev. Lett.* **50**, 1684 (1983).
- <sup>8</sup>For a general reference, see, e.g., S.T. Epstein in *The Force Concept in Chemistry*, edited by B.M. Deb (Van Nostrand Reinhold, New York, 1981), p. 241.
- <sup>9</sup>A.H. Zewail, *Femtochemistry, Ultrafast Dynamics of the Chemical Bonds* (World Scientific, Singapore, 1994), Vols. I and II.
- <sup>10</sup>See, e.g., E.K.U. Gross, J.F. Dobson, and M. Petersilka, in *Density Functional Theory II*, edited by R.F. Nalewajski (Springer-Verlag, Berlin, 1996), p. 97.
- <sup>11</sup>C. Kan, N.H. Burnett, C.E. Capjack, and R. Rankin, *Phys. Rev. Lett.* **79**, 2971 (1997).
- <sup>12</sup>N.H. Tolk, R.G. Albridge, A.V. Bernes, B.M. Bernes, J.L. Davidson, V.D. Gordon, G. Mergeritoudo, J.T. McKinley, G.A. Mensing, and J. Sturmman, *Appl. Surf. Sci.* **106**, 205 (1996).
- <sup>13</sup>D.L. Klein, P.L. McEuen, J.E.B. Katari, R. Roth, and A.P. Alivisatos, *Appl. Phys. Lett.* **68**, 2574 (1996).
- <sup>14</sup>M.A. Reed, C. Zhou, C.J. Muller, T.P. Burgin, and J.M. Tour, *Science* **278**, 252 (1997).
- <sup>15</sup>See, e.g., *Scanning Tunneling Microscopy III*, edited by R. Wiesendanger and H.-J. Güntherodt (Springer-Verlag, Berlin, 1993).
- <sup>16</sup>M. Di Ventra and S.T. Pantelides, *Phys. Rev. B* **59**, R5320 (1999); M. Di Ventra, S.T. Pantelides, and N.D. Lang, *Phys. Rev. Lett.* **84**, 979 (2000).
- <sup>17</sup>R. Landauer, *Phys. Rev. B* **16**, 4698 (1977); **14**, 1474 (1976).
- <sup>18</sup>See, e.g., R.S. Sorbello and B.B. Dasgupta, *Phys. Rev. B* **21**, 2196 (1980).
- <sup>19</sup>E.F. Hayes and R.G. Parr, *J. Chem. Phys.* **43**, 1831 (1965).
- <sup>20</sup>N.D. Lang, *Phys. Rev. B* **45**, 13 599 (1992); **49**, 2067 (1994).
- <sup>21</sup>A.C. Hurley, *Proc. R. Soc. London, Ser. A* **226**, 170 (1954); **226**, 179 (1954). See also Ref. 8.
- <sup>22</sup>P. Bala, B. Lesyng, and J.A. McCammon, *Chem. Phys. Lett.* **219**, 259 (1994); F.M. Fernández, *ibid.* **233**, 651 (1995).
- <sup>23</sup>See, e.g., K. Gottfried, *Quantum Mechanics* (Benjamin, New York, 1966), p. 66.
- <sup>24</sup>We consider here, for convenience, the elastic scattering case only. Inelastic scattering (e.g., phonons) can be readily introduced in the formulation as extra terms in the Hamiltonian (16).
- <sup>25</sup>S. Datta, W. Tian, S. Hong, R. Reifenberger, J.I. Henderson, and C.P. Kubiak, *Phys. Rev. Lett.* **79**, 2530 (1997).
- <sup>26</sup>H. Ness and A.J. Fisher, *Phys. Rev. B* **56**, 12 469 (1997), and references therein.
- <sup>27</sup>We stress, however, that at a fixed energy and for a given finite basis set, the scattering amplitudes satisfy stationarity principles that lead to either a minimum or a maximum [see, e.g., J.R. Taylor, in *Scattering Theory* (Wiley, New York, 1972), p. 273]. A minimum principle is guaranteed only when the spectrum of the Hamiltonian has *no* bound states.
- <sup>28</sup>Note that an analogous example has been investigated in Ref. 20 with similar results within the frozen-core approximation. The formulation presented in this paper gives a rigorous definition of the forces obtainable from such type of calculations.
- <sup>29</sup>N.D. Lang, *Phys. Rev. B* **52**, 5335 (1995).
- <sup>30</sup>We calculated the potential induced by the presence of the atom between the electrodes in a rectangular box of 8.2 Å along the direction perpendicular to the electrode surfaces and 6.3 Å in both directions parallel to the surfaces. We employed  $N=17$  grid points for the former direction and  $N=9$  for the other two in reciprocal space. The potential includes exchange-correlation terms that are treated in the local-density approximation. No long-range correlation terms are thus included and, in particular, Van de Waals forces.
- <sup>31</sup>The energy region  $\sigma$  has been divided into  $N=32$  intervals.
- <sup>32</sup>N.D. Lang and A.R. Williams, *Phys. Rev. B* **18**, 616 (1978).
- <sup>33</sup>W. Kohn and L.J. Sham, *Phys. Rev.* **140**, A1133 (1965).

## Temperature Effects on the Transport Properties of Molecules

M. Di Ventura,<sup>1,\*</sup> S.-G. Kim,<sup>1</sup> S. T. Pantelides,<sup>1,2</sup> and N. D. Lang<sup>3</sup>

<sup>1</sup>*Department of Physics and Astronomy, Vanderbilt University, Nashville, Tennessee 37235*

<sup>2</sup>*Solid State Division, Oak Ridge National Laboratory, Oak Ridge, Tennessee 37831*

<sup>3</sup>*IBM Research Division, Thomas J. Watson Research Center, Yorktown Heights, New York 10598*

(Received 25 July 2000)

Recent experiments found an unusual temperature-induced large shift in the resonant-tunneling voltage of certain molecules. We report first-principles calculations showing that such behavior can be caused by the excitation of rotational modes of ligands. These modes have classical characteristics, i.e., the maximum excursion is dominant, while at the same time they have a significant effect on the energy levels responsible for resonant tunneling. The proposed mechanism of ligand rotations is unique to molecules and accounts for the fact that the effect is not seen in semiconductor nanostructures.

DOI: 10.1103/PhysRevLett.86.288

PACS numbers: 73.40.Jn, 73.40.Cg, 73.40.Gk, 85.65.+h

Interest in the transport properties of single molecules is increasing due to their possible use as electronic components [1]. New synthetic reactions allow the realization of new and diverse molecules, resulting in devices with novel and unique properties [2]. For example, molecules have been shown to operate as Coulomb blockade structures [3], diodes [4], or switching devices with high negative differential resistance (NDR) even at room temperature [5,6]. Theoretical investigations have elucidated, e.g., the role of contact chemistry and geometry on the current-voltage characteristics of single molecules [7], molecule-length dependence of the conductance [8], role of the injection energy at the contacts [9], three-terminal device operation [10], and stress-induced modification of transport properties [11].

Molecules are intrinsically different from semiconductor nanostructures, and one expects that some of their transport properties would be unique. The recent report by Chen *et al.* [6] confirms that this is the case with the *temperature dependence* of the resonant-tunneling peak. The molecules studied by Chen *et al.* are chains of three benzene rings with one or more ligands attached to the carbon atoms of the central ring. An unusually sharp peak with an enormous NDR has been observed at very low temperatures [6]. At higher temperatures, the peak broadens, as expected, but it also shifts to substantially lower voltage [6]. The large shift ( $\sim 1$  V) is highly unusual and contrasts sharply with the well-known behavior of resonant tunneling in semiconductor heterostructures where practically no voltage shifts are observed [12,13]. Seminario *et al.* [14] have proposed that the voltage shift is caused by a rotation of the middle carbon ring plus charging of the molecule by single extra electrons. The suggestion was motivated by *ground-state* calculations of the electronic structure of the same molecule and *assumption* that the molecule's lowest-unoccupied molecular orbital (LUMO—in this case referred to as  $\pi^*$  orbital) mediates resonant tunneling. Our recent first-principles calculations [7] of transport in a single benzene ring have shown, however, that *the electronic structure of molecules changes substantially*

*as a function of applied voltage*, making it difficult to infer transport properties from ground-state electronic properties.

In this Letter we report first-principles calculations that explore the role of ligands in determining the transport properties of the benzene-ring family of molecules. The study was motivated by the fact that a three-benzene-ring molecule without ligands has effectively zero conductivity for all voltages (up to about 5 V) and insertion of ligands produces significant differences in the shape of the *I-V* curve [6]. As an additional indication we performed ground-state density-functional calculations [15] on the three-ring molecule which revealed that rotation of the middle ring produces no perceptible change in the electronic structure of the molecule in the vicinity of the highest-occupied molecular orbital (HOMO)-LUMO states, whereas rotation of the ligand does. Our full transport calculations for a single benzene ring with an NO<sub>2</sub> ligand find essentially the same behavior as that exhibited by the three-ring molecule measured by Chen *et al.* [6,16]: rotation of the ligand—activated by temperature—causes a substantial shift in the resonant-tunneling voltage. This large voltage shift is due in part to the rotation properties of the NO<sub>2</sub> group and in part to the different symmetry of the states localized on the NO<sub>2</sub> group with respect to the  $\pi$  orbitals of the carbon ring responsible for transport. In particular, unlike the  $\pi$  orbitals of the carbon ring, the orbitals on the NO<sub>2</sub> group have a nonzero dipole moment: they have a lower symmetry with respect to reflection through a plane bisecting the molecular axis so that they are shifted in energy by a field applied along the axis. The perturbation of the states induced by the external electric field is thus first order. At increasing temperature, these states thus “push” the  $\pi$  orbital to reach the resonant tunneling condition at lower voltages. The results show that, unlike in mesoscopic devices, temperature can produce different effects on resonant tunneling in molecular structures. This must be taken into account in the design of future molecular devices.

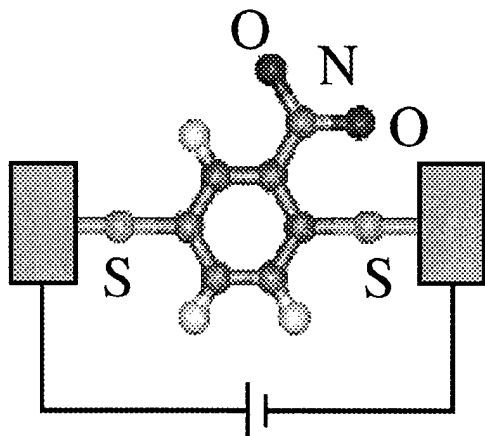


FIG. 1. Scheme of the molecular structure investigated. The structure is the benzene-1,4-dithiolate molecule where a H atom is replaced by a  $\text{NO}_2$  group. All atoms lie on the plane defined by the carbon ring. The sulfurs attach to ideal metallic leads.

The molecule we investigated is depicted in Fig. 1. The two sulfur atoms make contact to gold surfaces that we model with ideal metals (uniform positive background model or jellium model [17]). The interior electron density of the jellium electrodes is taken equal to the value for metallic gold ( $r_s \approx 3$ ). We computed the  $I$ - $V$  characteristic using the method developed in Ref. [18]. The electron wave functions are computed by solving the Lippman-Schwinger equation iteratively to self-consistency in steady state. Exchange and correlation are included in the density-functional formalism within the local-density approximation [18]. The current is computed from the wave functions of the electrode-molecule system. At zero temperature, the atoms of the  $\text{NO}_2$  group lie on the same plane defined by the six-carbon ring (see Fig. 1).

We first discuss the  $I$ - $V$  characteristics at zero temperature and then the effect of the rotation of the  $\text{NO}_2$  group. The calculated  $I$ - $V$  characteristic of the molecule is plotted in Fig. 2. The current is effectively zero for voltages up to about 0.5 V. The current then increases almost linearly with external bias until a peak and a valley are visible at about 3.8 and 4.2 V, respectively. This behavior can be understood by looking at the density of states (DOS) for different external voltages. In Fig. 3 we show the calculated DOS of the molecule for three different voltages, namely, 0.01, 3.8, and 4.2 V (the DOS shown is the difference between that of the molecule-electrodes system and that of the electrodes without the molecule). The zero of energy is the left Fermi level so that the right Fermi level is equal to the external bias (in Fig. 3 the labels  $E_{FR}$  correspond to the 3.8 and 4.2 V values of the bias). Contrary to the case of the benzene-1,4-dithiolate molecule (i.e., the same molecule with the  $\text{NO}_2$  group replaced by a H) the  $\pi$  bonding orbital of the carbon ring lies close to the left Fermi level (at about 0.5 eV below the left Fermi level for a bias of 0.01 V—see Fig. 3) [7]. This is due to the presence

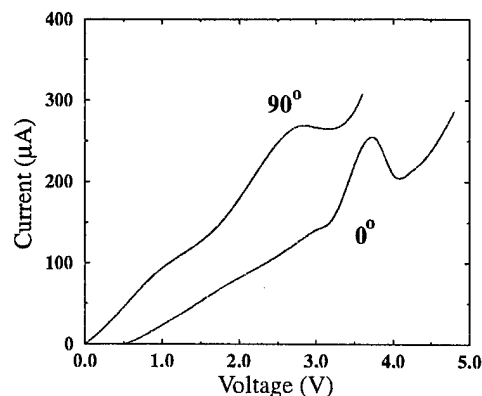


FIG. 2. Theoretical  $I$ - $V$  curve of the molecular structure of Fig. 1 for  $0^\circ$  and  $90^\circ$  of rotation of the  $\text{NO}_2$  group with respect to the carbon-ring plane.

of the hybridized  $p$  orbitals of nitrogen and oxygens that push the  $\pi$  orbital higher in energy. These states lie about 1.7 eV below the  $\pi$  orbital for a 0.01 V bias (indicated as  $\text{NO}_p$  in Fig. 3). Therefore, these states do not contribute directly to transport. Increasing the bias, the  $\pi$  orbital enters in resonance with the left Fermi level and a peak in the current occurs at this resonant tunneling condition. Increasing the bias further, the resonant tunneling condition is no longer satisfied and a valley in the  $I$ - $V$  curve is observed [19]. This is completely different from the case of the molecule without the  $\text{NO}_2$  group where the first resonant tunneling condition is due to  $\pi^*$  antibonding states [7]. We note that the resonant tunneling condition at zero temperature occurs at 3.8 V, i.e., at a higher voltage than in the experiment [6]. We note, however, that in the experiment three carbon rings form the entire molecule. In this case, the  $\pi$  orbitals of the outer rings will push the  $\pi$

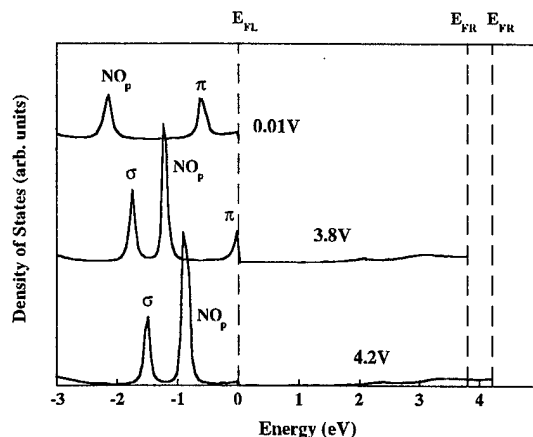


FIG. 3. Difference between the density of states of the two semi-infinite electrodes with and without the molecule of Fig. 1 in between, for three different voltages. The left Fermi level ( $E_{FL}$ ) has been chosen as the zero of energy. The labels  $E_{FR}$  correspond to the energy position of the right Fermi levels. The three curves correspond to the bias voltages indicated.

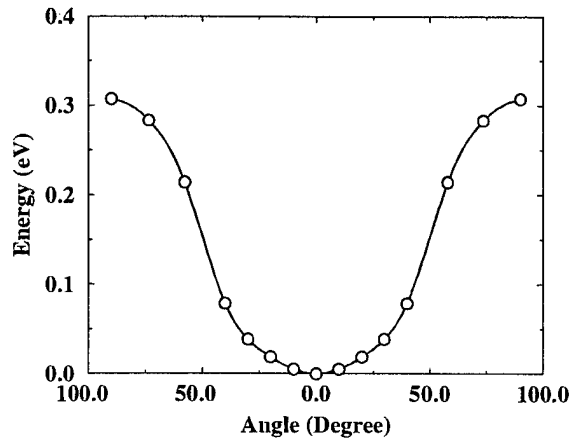


FIG. 4. Total energy of the isolated molecule of Fig. 1 for different angles of rotation of the  $\text{NO}_2$  group with respect to the carbon-ring plane.

orbital of the central ring even closer to the left Fermi level thus allowing resonant tunneling at lower voltage. Overall the molecule behaves as a molecular resonant tunneling device.

Let us now discuss the effects of temperature on the  $I$ - $V$  characteristics. Increasing the temperature, vibrational modes can be excited. However, usual optical-phonon scattering cannot account for the large shift of the current peak observed experimentally [13]. To confirm this, we performed a set of calculations of the current at external voltages close to the resonant tunneling condition where a "frozen phonon" has been allowed in the structure. We considered the highest frequency C-H vibrational mode, and we found that displacements of the H atoms along the C-H bond reduce the current but do not shift the voltage at which resonant tunneling occurs. On the other hand, the rotation of the  $\text{NO}_2$  group with respect to the plane of the carbon ring produces a different effect. This rotational mode can easily be activated by temperature. This is demonstrated in Fig. 4 where we plot the total energy of the free molecule for different rotation angles of the  $\text{NO}_2$  group with respect to the plane of the carbon ring [15]. The total energy difference between  $0^\circ$  and  $90^\circ$  of rotation is about 0.3 eV. An estimate of the energy level separation for this vibrational mode can be obtained by fitting the curve of Fig. 4 to a simple harmonic potential up to about  $50^\circ$  of rotation [20]. The energy levels are thus  $E_n = \hbar\omega(n + 1/2)$ ,  $n = 0, 1, \dots$ , and  $\omega = \sqrt{\kappa/I}$ . Here  $\kappa$  is obtained from a fit to a harmonic potential and  $I = 2M_O(d_{OO}/2)^2$  is the moment of inertia, where  $M_O$  is the mass of the oxygen and  $d_{OO}$  is the distance between the two oxygens of the  $\text{NO}_2$  group. Taking into account all parameters, the energy separation is about 3 meV. The  $\text{NO}_2$  group can thus rotate easily at room temperature, practically as a classical rigid rotator, and the system will spend most of the time at the highest degree of rotation possible at a given temperature. This rotation produces the same effect

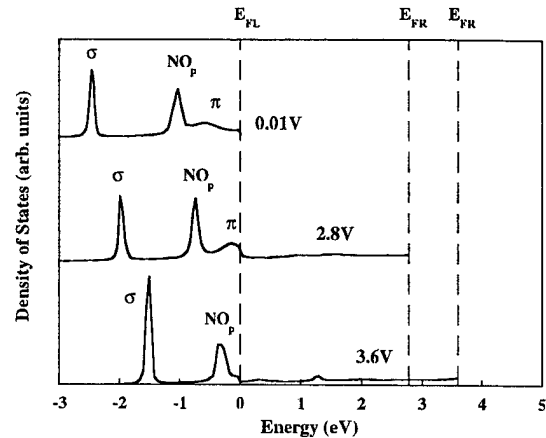


FIG. 5. Density of states for three different voltages for the molecule with the  $\text{NO}_2$  group rotated by  $90^\circ$  with respect to the carbon-ring plane. The same conventions apply as in Fig. 3.

on the  $I$ - $V$  characteristics as observed experimentally. This is shown in Fig. 2 for the  $90^\circ$  rotation. The peak-to-valley ratio is reduced, and the peak occurs at about 1 V less than at zero temperature. The reason for this can be rationalized by looking at the DOS for different external voltages. In Fig. 5 we plot the calculated DOS of the molecule with the  $\text{NO}_2$  group rotated by  $90^\circ$  for three different voltages, namely, 0.01, 2.8, and 3.6 V. The same conventions as in Fig. 3 apply. The rotation of the  $\text{NO}_2$  group pushes the NO-related  $p$  orbitals very close to the ring  $\pi$  orbital (the energy separation is now less than 0.5 eV). Because of symmetry, the dipole moment of the  $\pi$  orbital is zero while the dipole moment of the NO-related  $p$  orbitals is non-vanishing. Therefore, by applying an external electric field the NO-related  $p$  orbitals will be subject to a linear Stark shift while the ring  $\pi$  orbital shows a quadratic Stark shift [21]. Therefore, with increasing bias, the NO  $p$  orbitals get closer to the left Fermi level faster than the  $\pi$  orbital. Since, in the present case, the two orbitals are very close in energy, the  $\pi$  orbital of the benzene ring will be "forced" to reach the resonant tunneling condition at a lower bias due to the presence of the NO  $p$  orbitals. The effect is sizable since at  $90^\circ$  the voltage shift for the peak in the  $I$ - $V$  curve is about 1 V as observed in the experiment [6].

In conclusion, we have shown that thermally excited rotational modes of single molecules, like rotation of ligands, can have dramatic effects on their  $I$ - $V$  characteristics. The result has no counterpart in usual mesoscopic physics and must be taken into account in the design of future molecular devices.

We thank A. Tackett for some help in the development of the code used in the present work. This work was supported in part by the DARPA/ONR Grant No. N00014-99-1-0351, National Science Foundation Grant No. DMR-98-03768, the Division of Materials Sciences, U.S. Department of Energy under Contract No. DE-AC05-96OR2264 with Lockheed Martin Energy

Research Corp., and by the William A. and Nancy F. McMinn Endowment at Vanderbilt University. Some of the calculations have been performed on the IBM SP2 at the National Partnership for Advanced Computational Infrastructure at the University of Michigan.

---

\*Present address: Department of Physics, Virginia Polytechnic Institute and State University, Blacksburg, Virginia, 24061.

- [1] See, e.g., *Molecular Electronics: Science and Technology*, edited by A. Aviram and M. A. Ratner (New York Academy of Sciences, New York, 1998).
- [2] See, e.g., D. G. Gordon *et al.*, Proc. IEEE **85**, 521 (1997); J. K. Gimzewski and C. Joachim, Science **283**, 1683 (1999).
- [3] D. Porath and O. Milo, J. Appl. Phys. **81**, 2241 (1997).
- [4] E. W. Wong, C. P. Collier, M. Behloradsky, F. M. Raymo, J. F. Stoddart, and J. R. Heath, J. Am. Chem. Soc. **122**, 5831 (2000).
- [5] M. A. Reed, C. Zhou, C. J. Muller, T. P. Burgin, and J. M. Tour, Science **278**, 252 (1997).
- [6] J. Chen, M. A. Reed, A. M. Rawlett, and J. M. Tour, Science **286**, 1550 (1999).
- [7] M. Di Ventra, S. T. Pantelides, and N. D. Lang, Phys. Rev. Lett. **84**, 979 (2000).
- [8] S. Datta, W. Tian, S. Hong, R. Reifenberger, J. I. Henderson, and C. P. Kubiak, Phys. Rev. Lett. **79**, 2530 (1997); M. P. Samanta, W. Tian, S. Datta, J. I. Henderson, and C. P. Kubiak, Phys. Rev. B **53**, R7626 (1996).
- [9] S. N. Yaliraki, A. E. Roitberg, C. Gonzalez, V. Mujica, and M. A. Ratner, J. Chem. Phys. **111**, 6997 (1999).
- [10] M. Di Ventra, S. T. Pantelides, and N. D. Lang, Appl. Phys. Lett. **76**, 3448 (2000).
- [11] See, e.g., J. K. Gimzewski and C. Joachim, Science **283**, 1683 (1999).
- [12] V. J. Goldman, D. C. Tsui, and J. E. Cunningham, Phys. Rev. Lett. **58**, 1256 (1987).
- [13] N. S. Wingreen, K. W. Jacobsen, and J. W. Wilkins, Phys. Rev. Lett. **61**, 1396 (1988).
- [14] J. Seminario, A. G. Zacarias, and J. M. Tour, J. Am. Chem. Soc. **122**, 3015 (2000).
- [15] The total energy calculations have been done with a supercell geometry within density functional theory in the local density approximation [W. Kohn and L. J. Sham, Phys. Rev. **140**, A1133 (1965)].
- [16] The same effect has been observed with and without an NH<sub>2</sub> group that replaces a H of the central benzene ring opposite to the NO<sub>2</sub> group (see Ref. [6]).
- [17] See, e.g., N. D. Lang, in *Solid State Physics*, edited by F. Seitz, D. Turnbull, and H. Ehrenreich (Academic, New York, 1973), Vol. 28, p. 225.
- [18] N. D. Lang, Phys. Rev. B **52**, 5335 (1995); **49**, 2067 (1994).
- [19] Note that the peak in the DOS due to  $\pi$  orbital is no longer visible for voltages higher than the bias at which resonant tunneling occurs. This is due to the complete delocalization of the  $\pi$  orbital.
- [20] Note that this is not a free rigid rotator. Therefore, the lowest energy level does not have zero energy.
- [21] See, e.g., B. H. Bransden and C. J. Joachain, in *Physics of Atoms and Molecules* (Longman Group Limited, New York, 1983), p. 377.

## Current-Induced Forces in Molecular Wires

M. Di Ventra,<sup>1</sup> S. T. Pantelides,<sup>2,3</sup> and N. D. Lang<sup>4</sup>

<sup>1</sup>*Department of Physics, Virginia Polytechnic Institute and State University, Blacksburg, Virginia 24061*

<sup>2</sup>*Department of Physics and Astronomy, Vanderbilt University, Nashville, Tennessee 37235*

<sup>3</sup>*Solid State Division, Oak Ridge National Laboratory, Oak Ridge, Tennessee 37831*

<sup>4</sup>*IBM Research Division, Thomas J. Watson Research Center, Yorktown Heights, New York 10598*

(Received 7 June 2001; published 9 January 2002)

We report first-principles calculations of current-induced forces in molecular wires for which experiments are available. We investigate, as an example, the effect of current-induced forces on a benzene molecule connected to two bulk electrodes via sulfur end groups. We find that the molecule twists around an axis perpendicular to its plane and undergoes a “breathing” oscillation at resonant tunneling via antibonding states. However, current-induced forces do not substantially affect the absolute value of the current for biases as high as 5 V, suggesting that molecular wires can operate at very large electric fields without current-induced breakdown.

DOI: 10.1103/PhysRevLett.88.046801

PACS numbers: 73.40.Jn, 73.40.Cg, 73.40.Gk, 85.65.+h

The phenomenon of atom motion due to current flow (electromigration) has been extensively studied in the past both from the fundamental standpoint and for its importance in microelectronics [1–4]. Most recently, a new electronics is emerging that envisions the use of single molecules or molecular wires as fundamental components in electronic devices [5]. For instance, it has been demonstrated that molecules can operate as Coulomb blockade structures [6], transistors [7,8], diodes [9], or switching devices with high negative differential resistance even at room temperature [10–12]. Since electromigration has been a major concern in conventional microelectronics due to current-induced device breakdown, the question arises as to whether current-induced forces may present a severe limitation to the development of molecular electronics.

It was recognized in early theoretical work [1–4] that current-induced forces on a given physical system depend strongly on the microscopic details of the self-consistent electric field that is created upon scattering of the electrons across the region of interest. Self-consistency in the calculation of the local electric field with the correct scattering boundary conditions is thus essential to have meaningful quantitative results on current-induced forces.

In this Letter, we report first-principles calculations that explore the role of current-induced forces on molecular wires, and their role in weakening chemical bonds at the contacts and in the wire. Considering as an example current flow in a benzene molecule connected to two bulk electrodes via sulfur end groups [10], we extract general trends on the stability of molecular wires under current flow. The molecular structure investigated represents a prototype molecular device showing nonlinear transport properties [10]. It has been investigated both experimentally [10] and theoretically [13–16] without, however, addressing the issue of current-induced forces. Since we are interested in the role and magnitude of these forces, and the actual experimental contact geometry and structure of the molecular device are not known, we focus on the molecular

structure depicted in Fig. 1. The effect of contact chemistry and geometry in the current has been discussed in Ref. [13]. We find that, under current flow, the molecule twists around an axis perpendicular to its plane and undergoes a “breathing” oscillation at resonant tunneling via antibonding states [17]. However, current-induced forces do not substantially affect the absolute value of the current up to biases as high as 5 V. This is a remarkable result for a molecule of nominal length of only 8 Å. At external voltages larger than 5 V, the contact that is depleted of electrons during current flow weakens considerably with a consequent dramatic reduction of the current. This suggests that molecular wires can operate at very large biases without current-induced breakdown, in contrast to recent findings in atomic gold wires that have been found to break at biases of 1 to 2 V [18,19].

We computed the I-V characteristics of the molecular structure by using the method discussed in Ref. [20]. The two sulfur atoms of the molecule (see Fig. 1) make contact to gold surfaces that we model with ideal metals (jellium model) [20]. The interior electron density of the electrodes is taken equal to the value for metallic gold ( $r_s \approx 3$ ). The electron wave functions are computed by solving the Lippman-Schwinger equation iteratively to self-consistency in steady state. Exchange and correlation are included in

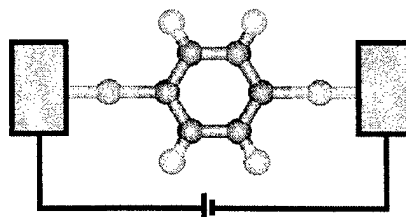


FIG. 1. Scheme of the molecular structure investigated. The structure is the benzene-1,4-dithiolate molecule. All atoms lie on the plane defined by the carbon ring. The sulfurs attach to ideal metallic leads.

the density-functional formalism within the local-density approximation [20]. The current is computed from the wave functions  $|\psi\rangle$  of the electrode-molecule system. The force  $\mathbf{F}$  acting on a given atom at position  $\mathbf{R}$  due to the electron distribution as modified by the external bias is given by the Hellmann-Feynman type of theorem developed in Ref. [21]:

$$\mathbf{F} = \sum_i \left\langle \psi_i \left| \frac{\partial H}{\partial \mathbf{R}} \right| \psi_i \right\rangle + \lim_{\Delta \rightarrow 0} \int_{\sigma} dE \left\langle \psi_{\Delta} \left| \frac{\partial H}{\partial \mathbf{R}} \right| \psi_{\Delta} \right\rangle. \quad (1)$$

The sum and integral in Eq. (1) include spin variables also. The first term on the right-hand side of Eq. (1) is the usual Hellmann-Feynman contribution to the force due to localized electronic states  $|\psi_i\rangle$ . The second term is the contribution to the force due to the continuum of states [21]. It is calculated by constructing, for each energy in the continuum, square-integrable wave functions  $|\psi_{\Delta}\rangle$  in an energy region  $\Delta$

$$|\psi_{\Delta}\rangle = \mathcal{A} \int_{\Delta} dE \psi, \quad (2)$$

where  $\mathcal{A}$  is a normalization constant and the  $\psi$ 's are single-particle wave functions in the continuum, solutions of the Lippmann-Schwinger equation [21]. The continuum integration  $\sigma$  covers the part of the spectrum occupied by the electrons at a given bias [22]. Finally, the total force on the atom includes a trivial ion-ion interaction. Starting from a given atomic configuration (e.g., the atoms at the equilibrium experimental atomic positions), we calculate the forces acting on each atom. We then move the atoms according to the gradient of these forces until the force on each atom is zero.

We now discuss the main results obtained using the above theoretical approach. The relaxed configuration of the system at zero bias consists of C-C bond lengths of 1.40 Å, C-H bond lengths of 1.09 Å, C-S bonds of 1.70 Å, and S-jellium surface bond length of 1.00 Å. The latter is in agreement with the equilibrium distance of sulfur adsorption on jellium surfaces [23], and the other bond lengths are in good agreement with the experimental bond lengths in isolated benzene molecules and thiophenol molecules [24].

The I-V characteristic of the molecular structure with and without the effect of current-induced forces is reported in Fig. 2. The first peak in conductance (indicated as a vertical arrow in Fig. 2) occurs at about 2.4 V and is due to resonant tunneling via  $\pi^*$  antibonding states (see also Ref. [13]). The second peak at about 4.4 V (also indicated as a vertical arrow in Fig. 2) is due to resonant tunneling via  $\pi$  bonding states [13]. The electron transport via antibonding states corresponds to a depletion of charge in the central C-C bonds, and an accumulation of charge in the nearest C-C bonds (see Fig. 3a). The total charge depleted with respect to the zero bias condition is about 0.05e per bond. This charge is nearly completely recov-

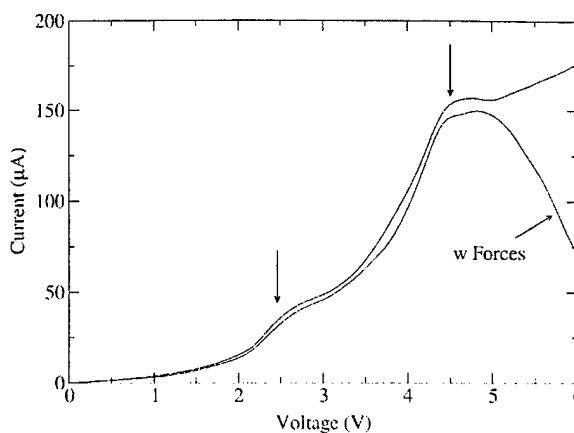


FIG. 2. Theoretical I-V curve of the molecular structure of Fig. 1 with and without the effect of current-induced forces. The vertical arrows indicate the onset of resonant tunneling via antibonding (at  $\sim 2.4$  V) and bonding (at  $\sim 4.4$  V) states.

ered in the middle bonds when the resonant tunneling condition is lost. In particular, at 4.4 V—corresponding to resonant-tunneling via  $\pi$  bonding states—the charge is

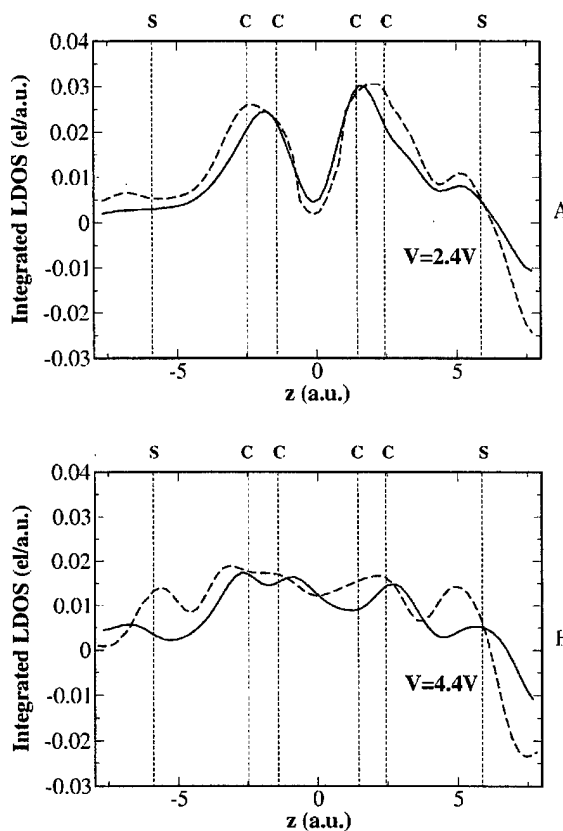


FIG. 3. Local density of states difference between that of the molecule-electrodes system and that of the electrodes without the molecule, integrated between left and right Fermi levels for a bias of 2.4 V (A) and 4.4 V (B). Solid lines correspond to the unrelaxed geometry, dashed lines to the relaxed one. The vertical dotted lines correspond to the unrelaxed atomic positions.

more uniformly distributed across all bonds in the benzene ring (see Fig. 3b).

It is immediately evident from Fig. 2 that current-induced forces do not substantially alter the absolute value of the current for external voltages as high as 5 V. Nonetheless, the molecular structure undergoes some structural transformations (see below).

The bonding and antibonding nature of the states involved in the electron scattering has a dramatic effect on the dynamics of the molecule under current flow. This is illustrated in Fig. 4 for different external biases. The structure at 0 V has been found to be unstable under current flow (see Fig. 4): With increasing bias, the mirror symmetry with respect to a plane perpendicular to both the benzene ring plane and the surface of the electrodes can be easily broken, leading to a slight rotation of the central carbon ring with respect to an axis perpendicular to its plane [17]. At the same time, the S-metal bond on the right electrode weakens due to the transfer of charge from the right to the left electrode (the left electrode is at a positive bias with respect to the right electrode, see Fig. 3a). At about 2.4 V, i.e., when resonant tunneling via antibonding states occurs, some charge depletes from the central C-C bonds, leading to a weakening of these bonds. Consequently, these bonds slightly expand forcing the remaining C-C and C-S bonds to expand. These bonds expand on average 0.05 Å while the C-H bonds are not affected. This can be rationalized by knowing that the  $\pi^*$  states of the molecule are formed only by carbon and sulfur  $p$  orbitals that are perpendicular to the ring plane, while the C-H bonds are  $\sigma$ -like. Upon relaxation, some extra charge is depleted from the central C-C bonds with consequent redistribution in the nearby bonds (see Fig. 3a, dashed line).

Increasing the bias further, the resonant-tunneling condition is lost and charge is almost completely recovered in the central C-C bonds (see Fig. 3). The C-C bonds then contract back to almost their length at 0 V. In summary, the molecule undergoes a “breathing” oscillation when the bias is scanned across the first resonant-tunneling condition. This “breathing” oscillation as a function of bias is typical only of resonant-tunneling via antibonding states. Indeed, increasing the bias further, until resonant-tunneling via bonding states is satisfied ( $\sim 4.4$  V), no bond-length oscillations are observed due to a more uniform distribution of charge across the central C ring (see Fig. 3b). On the other hand, with increasing bias, the central ring continues to twist with respect to an axis perpendicular to its plane, while the S-metal bond on the right electrode weakens (see

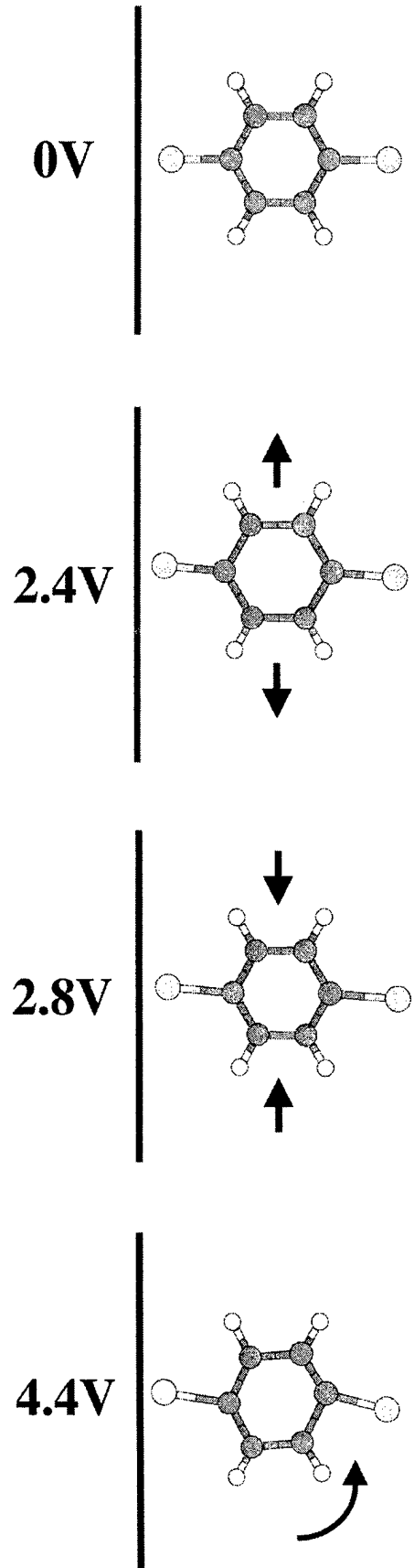


FIG. 4. Structural transformations of the molecule of Fig. 1 for four external biases. At 2.4 V, the C-C bonds of the molecule slightly expand, while at 2.8 V, the same bonds contract, as indicated by the arrows. Upon symmetry breaking, a counterclockwise (or, equivalently, a clockwise) rotation of the central carbon ring with respect to an axis perpendicular to its plane is observed. The left electrode is at a positive bias with respect to the right electrode.

Fig. 3b, dashed line). Remarkably, the absolute value of the current depends only weakly on the dynamical changes of the molecule for voltages up to about 5 V (see Fig. 2). At these high voltages, however, the charge transfer from the right to the left electrode strongly weakens the S-metal bond on the right electrode. This bond expands by more than 0.3 Å for biases larger than 5 V (at 6 V the bond expansion is 0.5 Å), therefore behaving as an extra barrier for electrons to tunnel across the molecular structure. The sign of the current-induced forces on the S atom of this bond coincide with the sign of the electron current [25]. Because of thermal and current fluctuations, and the fact that the S-metal bond has been weakened, the S-metal bond distance can oscillate at these high voltages, giving rise to small oscillations in the conductance [26]. Small conductance oscillations are indeed observed for such high voltages in the present system [10]. It is also worth noticing that complete fracture of this bond can occur at these high voltages if temperature effects are taken into account [19].

In conclusion, we have shown, using first-principles calculations, that current-induced forces in molecular devices can induce unusual dynamical changes in the structure of the molecules. However, we have found that the absolute value of the current is quite unaffected up to external voltages as high as 5 V, in contrast to the case of atomic gold wires that break at smaller biases: The strong  $\sigma$  bonds of the carbon-based molecular structures make them more resistant to current-induced forces than atomic gold wires.

This work was supported in part by DARPA/ONR Grant No. N00014-99-1-0351, NSF Grant No. DMR-98-03768, Oak Ridge National Laboratory, managed by UT-Battelle, LLC, for the U.S. DOE, and by the William A. and Nancy F. McMinn Endowment at Vanderbilt University.

- [1] R. Landauer and J. W. F. Woo, *Phys. Rev. B* **10**, 1266 (1974).  
 [2] A. K. Das and R. Peierls, *J. Phys. C* **8**, 3348 (1975).  
 [3] L. J. Sham, *Phys. Rev. B* **12**, 3142 (1975).  
 [4] R. S. Sorbello, *Solid State Phys.*, edited by H. Ehrenreich and F. Spaepen (Academic Press, New York, 1997), Vol. 51, p. 159; and references therein.  
 [5] See, e.g., *Molecular Electronics: Science and Technology*, edited by A. Aviram and M. A. Ratner (New York Academy of Sciences, New York, 1998).  
 [6] D. Porath and O. Milo, *J. Appl. Phys.* **81**, 2241 (1997).  
 [7] H. Park, J. Park, A. K. L. Lim, E. H. Anderson, A. P. Alivisatos, and P. L. McEuen, *Nature (London)* **407**, 57 (2000).  
 [8] M. Di Ventra, S. T. Pantelides, and N. D. Lang, *Appl. Phys. Lett.* **76**, 3448 (2000).  
 [9] E. W. Wong, C. P. Collier, M. Behloradsky, F. M. Raymo, J. F. Stoddart, and J. R. Heath, *J. Am. Chem. Soc.* **122**, 5831 (2000).

- [10] M. A. Reed, C. Zhou, C. J. Muller, T. P. Burgin, and J. M. Tour, *Science* **278**, 252 (1997).  
 [11] J. Chen, M. A. Reed, A. M. Rawlett, and J. M. Tour, *Science* **286**, 1550 (1999).  
 [12] M. Di Ventra, S.-G. Kim, S. T. Pantelides, and N. D. Lang, *Phys. Rev. Lett.* **86**, 288 (2001).  
 [13] M. Di Ventra, S. T. Pantelides, and N. D. Lang, *Phys. Rev. Lett.* **84**, 979 (2000).  
 [14] E. G. Emberly and G. Kirczenow, *Phys. Rev. B* **58**, 10911 (1998).  
 [15] M. P. Samanta, W. Tian, S. Datta, J. I. Henderson, and C. P. Kubiak, *Phys. Rev. B* **53**, R7626 (1996).  
 [16] S. N. Yaliraki, A. E. Roitberg, C. Gonzalez, V. Mujica, and M. A. Ratner, *J. Chem. Phys.* **111**, 6997 (1999).  
 [17] At biases other than zero, the symmetric structure with mirror symmetry with respect to a plane perpendicular to both the benzene ring plane and the surface of the electrodes, has been found to have higher total energy than the same structure with broken symmetry. This symmetry can, therefore, be broken by any external perturbation, such as, e.g., thermal vibrations and/or structural irregularities at the contacts, leading to a rotation of the molecule. Both clockwise and counterclockwise rotations are equally probable. This instability and consequent small rotation (less than 5° even at 5 V) is mostly due to the weakening and expansion of the S-right-electrode bond and to the fact that the electrodes do not expand. The result would be the same if atomic electrodes were used since very small relaxations are expected for the electrode atoms (see, e.g., Ref. [19]).  
 [18] H. Yasuda and A. Sakai, *Phys. Rev. B* **56**, 1069 (1997).  
 [19] T. N. Todorov, J. Hoekstra, and A. P. Sutton, *Phys. Rev. Lett.* **86**, 3606 (2001).  
 [20] N. D. Lang, *Phys. Rev. B* **52**, 5335 (1995); **49**, 2067 (1994); M. Di Ventra and N. D. Lang, *Phys. Rev. B* **65**, 045402 (2002).  
 [21] M. Di Ventra and S. T. Pantelides, *Phys. Rev. B* **61**, 16 207 (2000).  
 [22] The energy region  $\sigma$  has been divided into  $N = 128$  energy intervals. Convergence in the forces has been checked by increasing  $N$ . Plane waves have been chosen to represent the Hilbert space (see Ref. [21]).  
 [23] N. D. Lang, S. Holloway, and J. K. Nørkov, *Surf. Sci.* **150**, 24 (1985).  
 [24] Y. Takata *et al.*, *Surf. Sci.* **259**, 266 (1991).  
 [25] We want to stress that the sign of current-induced forces might not be necessarily the same for different bond structures. It is also not always possible to predict *a priori* the sign of current-induced forces with respect to the electron flow (see, e.g., Refs. [4,19–21]).  
 [26] Because of the large vibrational frequencies of the molecule investigated and its small feature length, we expect in this case that heating effects take place mostly in the electrodes for biases at which breathing occurs. For larger biases, local heating of the molecular region can contribute to the S-metal bond oscillations as well as to steady-state current fluctuations. However, the reduction of the current due to the S-metal bond weakening is large enough for biases greater than 5 V that this effect should be observable even in the presence of current fluctuations.